R. & M. No. 3329

MINISTRY OF AVIATION

AERONAUTICAL RESEARCH COUNCIL
REPORTS AND MEMORANDA

Wind-Tunnel Experiments on a Rectangular-Wing Jet-Flap Model of Aspect-Ratio 6

By A. J. ALEXANDER and J. WILLIAMS

LONDON: HER MAJESTY'S STATIONERY OFFICE
1964
PRICE 15*s.* 0*d.* NET

Wind-Tunnel Experiments on a Rectangular-Wing Jet-Flap Model of Aspect-Ratio 6

By A. J. ALEXANDER and J. WILLIAMS*

Reports and Memoranda No. 3329†
June, 1961

Summary.

Balance measurements of lift, pitching moment and thrust on an aspect-ratio 6 half-model wing and body in the N.P.L. 13 ft × 9 ft Wind Tunnel are discussed, and compared with theoretical estimates. The experimental investigation concentrated mainly on full-span flap deflections and blowing (with body cut-out), firstly without a tail unit, and then with a tailplane of variable incidence and height added to derive the mean downwash angles at a conventional fore-and-aft location. The effects of slot blockage and of part-span flaps on lift and thrust were also examined briefly.

LIST OF CONTENTS

* Both authors were on the staff of the Aerodynamics Division, National Physical Laboratory, when the experiments were started, but subsequently moved to the College of Aeronautics and the Royal Aircraft Establishment respectively.

† Replaces A.R.C. 22,947.

---

1. *Introduction.*

The first three-dimensional jet-flap experiments carried out at the N.P.L.[3] in 1953 were intended to demonstrate quickly the order of magnitude of finite aspect-ratio effects, being made on a small-scale pressure-plotting model of rectangular planform, mounted with an end plate at one end to give an effective aspect-ratio of nearly three. They were directly complementary to National Gas Turbine Establishment two-dimensional tests[1, 2] in that the models were basically of the same size (8 in. chord, 12 in. span), shape ($12\frac{1}{2}\%$ thick ellipse) and general construction, with trailing-edge-slot blowing. The total force on the model was of necessity derived by adding the still-air jet reaction at the nozzle to the pressure force felt by the aerofoil due to the mainstream flow over its external surface. The results showed that the spanwise distribution of pressure-lift loading induced by full-span blowing was not far different from that for a conventional wing at incidence, while conventional aspect-ratio corrections for pressure lift and pressure drag roughly continued to apply at values of the sectional momentum coefficient C_μ' below unity.

It was realised early on that, to facilitate variation of the jet angle to the mainstream in practice, the air might profitably be ejected from a slot located forward of the trailing edge so as to cling to the upper surface of a small T.E. flap. Some comparative pressure-plotting experiments at N.P.L. on further small-scale models[4], under nominally two-dimensional conditions, also confirmed that such a flap of about 10% chord would contribute a useful lift increment since boundary-layer control (B.L.C.) at the flap knee would be provided automatically by the jet efflux. However, the associated reduction in thrust arising from jet skin friction over the flap upper surface could not readily be ascertained with such models.

To follow up these exploratory studies, more comprehensive and elaborate experiments were then planned on a much larger half-model, with a wing of rectangular planform, variable aspect-ratio (3, 6, 9) and 12% thick RAE 104 section, the air being ejected over a 10% chord T.E. flap. These tests were intended[5] as part of an extensive fundamental investigation of three-dimensional effects for jet-flap wings, and to provide basic aerodynamic data then urgently needed for the design of the Hunting jet-flap research aircraft. Unfortunately, because of staff changes*—not experimental difficulties—the wing alone (without body) was never tested, while the effects of variation of aspect-ratio had to be studied on an R.A.E. complete model instead[8, 9].

Balance measurements of lift, pitching moment and thrust, together with some flow visualisation and jet traversing, were completed on the aspect-ratio 6 version of the half-model wing and body in the N.P.L. 13 ft × 9 ft Tunnel during 1957. This investigation mainly concentrated on full-span

---

* See footnote on first page of this report.

flaps and blowing (with body cut-out), firstly with the tail unit off, and then with a tailplane of variable angle and height to derive the mean downwash angles at a conventional fore-and-aft tailplane location. A few balance measurements were also carried out with slot blockage and with part-span flaps to simulate part-span blowing or a possible engine-cut condition. The present report supersedes and supplements brief 'Interim Notes' issued in early 1958[6]. Other tests, with variation of the chordwise extent of the T.E. flap and the wing nose shape have since been made on this model by M. N. Wood at R.A.E., Farnborough, but these reults are being reported separately[7].

2. *Experimental Method.*

2.1. *Model and Test Arrangement.*

The half-model of an untapered wing with body was hung upside-down from an overhead three-component balance, with a clearance of about 0·2 in. between the body centre-plane and a vertical false wall (reflection plate) mounted along wind in the working section of the N.P.L. 13 ft × 9 ft Tunnel (*see* Fig. 1a). A plan view of the 60 in. span half-model is shown in Fig. 1b. The wing had a 12% thick RAE 104 section of 20 in. chord, giving an effective aspect-ratio of 6, tip-to-tip. The plain T.E. flap was of 2 in. chord ($c_f/c = 0{\cdot}10$), aft of the flap hinge-line, with a spanwise extent of 54 in. measured from the wing-body junction to the wing tip. The model pitching axis was located 7 in. ($0{\cdot}35c$) aft of the wing leading-edge, but was offset 1·875 in. vertically upwards from the mean chord-line for structural reasons.

The wing comprised a large metal duct of rectangular chordwise section, to feed the air spanwise from the model root. This was connected by a spanwise row of large holes to a smaller duct which tapered chordwise to feed the blowing slot (Fig. 1b)*. The large duct was fitted with a wooden nose and sheathed with wood on its upper and lower surfaces to obtain the prescribed aerofoil shape over the front of the wing. The body was made from wood, hollowed out to reduce weight and to allow the T.E. flap to extend inside, the front and rear portions being of different lengths and interchangeable. Originally, it was intended to test the model without as well as with a body, to examine a foreplane as well as a tailplane arrangement, and to vary the wing aspect-ratio.

Compressed air was fed into the wing along the model pitching axis, through an air-bearing connector specially devised to avoid constraints on the model and balance, and to resist extraneous side-forces (*see* Ref. 14, Paragraph 3 and Appendix II). This connector was mounted in the tunnel working-section, but on the opposite side of the false wall from the model. Shielding from the airstream proved unnecessary, as the tare corrections due to the wind forces on the connector were relatively small and readily measurable (*see* Appendix). The air fed into the model was ejected from a slot 0·080 in. wide ($A_l/S' = 0{\cdot}004$) in the main wing at 90% chord as shown in Fig. 1b. For most of the tests the *mean-line* of the jet was arranged to be tangential to the upper surface of the flap nose, to ensure full deflection at large flap angles. The slot extent inside the body was sealed up throughout the present series of tests.

The rate of air ejection was controlled by reference to the static pressure in the main blowing duct, measured at 4 spanwise stations; this was about 5% less than the total head in the slot throat (relative to atmospheric) measured at zero mainstream speed. The spanwise variation of total head

* Provision was made to incorporate a throttling plate of many small holes between the two ducts, to modify the resulting spanwise distribution of pressure as necessary, but the spanwise uniformity of blowing proved satisfactory without this.

was less than $\pm$ 5% of the mean total head. The mass-flow rate to the slot was determined from the pressure difference across orifice plates inserted in straight pipes leading to the air-bearing connector, the correction for the leak of air from the connector being less than 1% for pressure ratios greater than 1·1 across the slot. The temperature of the compressed air was only a few degrees different from that of the tunnel mainstream, this difference being negligible for the determination of the momentum coefficient.

The tailplane used in these tests as a downwash meter had a rectangular planform of effective aspect-ratio 3, a planform area $S_T = 0{\cdot}25S$, and the same RAE 104 aerofoil section as the main wing. It was carried on a simple rectangular fin, with its quarter-chord point located 61·5 in. downstream of the main wing quarter-chord ($l/c = 3{\cdot}1$).

The techniques employed for ensuring a satisfactory mainstream flow past the model in the modified tunnel and for determining the tare forces associated with the system are briefly discussed in the Appendix.

2.2. *Reduction of Observations.*

The lift, pitching-moment and thrust coefficients have been evaluated from the corresponding balance measurements as follows, conventional corrections[16] being applied to allow for boundary 'lift-constraint' effects. The pitching moments are referred to the pitching axis of the model, which was at 35% chord in the present experiments and represents a possible c.g. position for a practical jet-flap aircraft.

$$C_L = (\text{measured lift})/q_0 S$$

$$C_m = (\text{measured moment})/q_0 Sc \ldots \text{tail-off}$$

or $$(\text{measured moment})/q_0 Sc - 0{\cdot}57(\partial C_m/\partial \alpha_T) C_L \ldots \text{tail-on}$$

$$C_T = (\text{measured thrust})/q_0 S - 0{\cdot}0105 C_L^2$$

$$\alpha^\circ = (\text{geometrical incidence}) + 0{\cdot}60 C_L \text{ degrees.}$$

The corrected mean downwash at the tailplane, relative to the body centre-line is

$$\epsilon^\circ = (\text{measured downwash}) + 1{\cdot}17 C_L \text{ degrees.}$$

It should be added that, after the reduction of observations and the preparation of diagrams for this report were completed, modified corrections for use with jet-flap models were derived by Maskell at the R.A.E.[12, 15]. The differences between the two types of corrections, when applied to results from the present range of tests are not significant, but they could be serious for larger values of the momentum coefficient or smaller aspect ratios.

The sectional momentum coefficient $C_\mu' \equiv M_J V_J / q_0 S'$ used here for the correlation of results has been evaluated from the measured mass-flow rate M_J (slugs/sec) and the theoretical velocity V_J(ft/sec) reached on isentropic expansion from the total pressure at the slot throat to the mainstream static pressure[14, 9]. The overall jet momentum coefficient $C_\mu \equiv M_J V_J / q_0 S$, used for comparing different spanwise extents of blowing, is based on the gross wing area S in the same way as usual wing force coefficients and is given by $0{\cdot}9 C_\mu'$ for full-span blowing (with body cut-out).

Before discussing the wind-on tunnel results, some wind-off measurements of the 'static jet-reaction' J and of the jet angle θ are worth mention. Unfortunately, the jet traverses feasible in the short time available proved inadequate for a quantitative momentum analysis.

2.3. *Static Jet-Reaction Measurements.*

With the flap on and at zero deflection ($\eta = 0°$), the ratio $J/M_J V_J$ measured wind-off was about $0{\cdot}85$ for pressure ratios p_D/p_0 between about $1{\cdot}1$ and $1{\cdot}7$*. The value $0{\cdot}85 M_J V_J$ can therefore be expected to be more closely representative of the jet momentum leaving the wing trailing-edge, at least wind-off. However, for the specification of jet angle θ, visual and total-head explorations of the jet are best employed, since estimates from static force measurements can be unreliable due to tunnel-wall constraint effects. The inclination of the flap upper surface to the chord-line was $+ 8°$ The jet direction, as measured by a thin streamer near the trailing-edge, was inclined at roughly $- 3°$ to this for all flap angles, giving the inclination of the jet to the chord-line as about 5°. Total-head traverses of the jet, at $\eta = 0°$ only, gave the inclination of the line of maximum total head to the chord-line as $7{\cdot}4°$, independent of blowing pressure. The line of mean total head was likewise inclined at $6{\cdot}5°$ for p_D/p_0 of $1{\cdot}1$ falling to $6{\cdot}0°$ for p_D/p_0 of $1{\cdot}7$. A value of $\theta \simeq \eta° + 7°$ has been used for comparative calculations in this report.

On the basis of these and subsequent R.A.E. tests[7, 9], the deficiency in J relative to $M_J V_J$ at small flap angles can be mainly attributed to the following; skin-friction drag due to the high-speed jet over the flap upper surface ($\simeq 0{\cdot}06 M_J V_J$); form drag due to the mainstream flow induced locally over the rearward facing part of the main wing ($\simeq 0{\cdot}01 M_J V_J$); losses due to jet impingement on the flap nose ($\simeq 0{\cdot}03 M_J V_J$); spacer drag ($\simeq 0{\cdot}01 M_J V_J$); inadequate estimates of V_J due to slot boundary layers ($\simeq 0{\cdot}04 M_J V_J$). With large flap angles, extra mixing and turning losses may be introduced, while the effective pressure ratio across the nozzle may be increased due to the local reduction in pressure at the curved flap knee. With the flap off, the ratio $J/M_J V_J$ remained at approximately $0{\cdot}93$ for p_D/p_0 values between $1{\cdot}1$ and $1{\cdot}7$, some deficiency additional to slot boundary-layer losses and spacer drag being present because of base drag where the flap had been removed.

2.4. *Range of Tests.*

Mainstream speeds of both 108 ft/sec ($R = 1 \times 10^6$) and 55 ft/sec were used†, the available duct pressures up to 10 p.s.i. gauge ($p_D/p_0 = 1{\cdot}7$) then permitting C_μ'-values up to about $0{\cdot}6$ and $2{\cdot}4$ respectively. The balance measurements tail-off were made over the incidence range $\alpha = - 8°$ to 20°, at several prescribed values of C_μ', with flap angles $\eta = 0°$, 30°, 60° and 90°, the corresponding jet angle $\theta°$ at the trailing edge being approximately 7° higher (*see* Section 2.3). Tests at more closely spaced intervals of C_μ' were made for each of the fixed incidences $- 8°$, $- 4°$, 0°, $+ 4°$, $+ 8°$. The effects of blocking in turn the inboard and outboard halves of the slot, of blocking the slot in alternate quarters to simulate an engine-cut case, of deflecting only the inboard flap, and of lowering the flap nose below the mean-line of the jet were investigated at zero incidence only.

The mean-downwash tests were carried out for the three tailplane heights $h = 24$ in., 18 in., 6 in. ($h/c = 1{\cdot}2$, $0{\cdot}9$, $0{\cdot}3$) above the model centre-line, and were restricted to incidences below the wing stall. The tailplane angles α_T were chosen at 2° intervals over a range of 12° to straddle the angle corresponding to the mean downwash.

* Corresponds to values to values of V_J between 400 ft/sec and 950 ft/sec.

† These corresponded to nominal tunnel speeds of 100 ft/sec and 50 ft/sec.

3. *Experimental Results.*

3.1. *Lift Increments at Constant Incidence.*

The variation of lift with momentum coefficient at small wing incidence ($\alpha = 0°$ and $-4°$) is shown in Fig. 2a for the flap angles $\eta = 0$, 30°, 60° and 90°, i.e. for jet deflections $\theta \simeq 7°$, 37°, 67°, 97°. Confirming the earlier exploratory pressure-plotting experiments[2, 3], the total lift coefficient C_L represented a considerable magnification of the direct jet-reaction lift $C_\mu'(S'/S)\sin(\theta+\alpha)$ from the corresponding vertical component of the jet momentum, because of the additional pressure lift generated on the wing surface. Typically, with $\alpha = 0°$ and $\eta = 60°$, a C_L-value of 5 was reached for C'_μ of only 1·8, giving a lift magnification factor $[(C_L/C_\mu')(S'/S)\sin(\theta+\alpha)]$ of about 4. Except at low C'_μ-values, the lift increments ΔC_L due to T.E. flap deflection and blowing were roughly proportional to the jet angle. The initial rapid rise in ΔC_L with small amounts of blowing can of course be attributed to the prevention of flow separation over the deflected T.E. flap by boundary-layer control. To ensure attached flow, C_μ'-values of about 0·012, 0·047 and 0·23 were required with $\eta = 30°$, 60° and 90° respectively; these were somewhat larger than for normal B.L.C. applications, because the wide slot designed here for jet-flap application led to blowing velocities barely exceeding the mainstream velocity at these small C_μ'-values.

To facilitate comparison with theory, the lift increment $\Delta C_{L\infty}$ for a corresponding two-dimensional aerofoil ($A = \infty$) has been estimated from the present experimental ΔC_L-values by writing

$$\Delta C_L(A,\, C_\mu') = \Delta C_{L\infty} F(A,\, C_\mu')\,\frac{S'}{S}.$$

The function

$$F(A,\, C_\mu') \simeq \frac{A + [2C_\mu'/\pi]}{A + 2 + 0{\cdot}604(C_\mu')^{1/2} + 0{\cdot}876C_\mu'}$$

is Maskell's theoretical correction factor for finite aspect-ratio effects on lift[11], while S'/S represents a crude part-span factor to allow for body cut-out. For this correlation, the value of C_μ' is taken to be that corresponding to the jet momentum leaving the flap trailing-edge, roughly 0·85 of the slot value based on measured mass-flow rate M_J and isentropic theoretical velocity V_J, while the jet angle θ is assumed 7° greater than the nominal flap angle η. Fig. 2b compares the resulting 'two-dimensional' empirical values both with the estimate $(\partial C_L/\partial\theta)_\infty\theta$ by Spence's linearised theory[10] and a modified estimate $[(1+t/c)(\partial C_L/\partial\theta)_\infty - C_\mu' t/c]\theta$ incorporating a crude allowance for the effect of wing section thickness/chord ratio t/c on the pressure lift. The experimental results and theory agree reasonably well, except at small C_μ'-values particularly when flow separation was present on the flap, or except for very large flap angles when a small-angle theory is certainly inadequate.

3.2. *Variation of Lift with Incidence.*

Lift-incidence curves at C_μ'-values of 0, 0·1, 0·4, 0·6, 0·95 and 2·3 are plotted in Fig. 3. For $\eta = 0°$ and 30°, $\partial C_L/\partial\alpha$ rose from about 0·07/deg without blowing to 0·12/deg when $C_\mu' = 2{\cdot}3$. For $\eta = 60°$, the increase was only slightly less, but for $\eta = 90°$ no significant increase occurred because of the extensive flow separation present over the front of the wing even at zero incidence. The stalling incidence fell some 2° when η was increased from 0° to 30°, or 3° when η was increased to 60° or more. Further losses of greater magnitude occurred when a small amount of blowing was applied ($C_\mu' \simeq 0{\cdot}1$), but at large C_μ' the stalling incidence recovered to that for the plain wing

except at $\eta = 90°$. The addition of transition wires at $0{\cdot}01c$ from the leading-edge on both surfaces, or of strips of distributed roughness, caused changes in C_L of less than $0{\cdot}1$ throughout the test range.

Some 'two-dimensional' empirical values for lift-incidence curve slopes $(\Delta C_L/\Delta\alpha)_\infty \equiv (\Delta C_L/\Delta\alpha)/\nu F$ have again been derived by introducing Maskell's aspect-ratio correction factor F, together with a part-span factor ν to allow for body cut-out*. Fig. 3e compares these values with the estimate $(\partial C_L/\partial\alpha)_\infty$ given by linearised theory and a modified estimate $[(1+t/c)(\partial C_L/\partial\alpha)_\infty - C_\mu' t/c]$ incorporating a thickness correction on the wing pressure-lift contribution, the trailing-edge C_μ' again being assumed to be $0{\cdot}85$ of the prescribed slot value. Clearly, for jet deflections of 60° or more, the predicted values are far too high because flow separation then began to develop over the wing nose even at small incidences.

3.3. *Pitching Moments and Trimming.*

Curves of pitching moment against lift at constant values of C_μ' or α are shown in Fig. 4†, referred to the model pitching axis at $0{\cdot}35c$. The aerodynamic centre of the plain wing and body ($\eta = C_\mu' = 0$) was about $0{\cdot}19c$ behind the wing leading-edge and, in contrast to theoretical trends, moved aft with increasing C_μ' when $\eta \leqslant 30°$. For example, at incidences well below the stall when $\eta = 30°$, the aerodynamic centre moved from $0{\cdot}22c$ to $0{\cdot}28c$ as C_μ' was raised from 0 to $2{\cdot}3$, in contrast to the forward shift predicted by linearised theory[10]. Unfortunately, a reliable analysis at larger flap angles was not feasible, because the variation of C_m with C_L was irregular due to the presence of flow separations over the wing nose even at small incidences. Although the stall was unstable, except at small flap angles and C_μ', it rarely became severe.

The centre of lift again generally moved rearward as C_μ' increased or as α decreased with C_μ' constant. For example, with $\alpha = 0°$ and $\eta = 30°$, the centre of lift moved from $0{\cdot}45c$ to nearly $0{\cdot}75c$ as C_μ' was raised from 0 to $2{\cdot}3$, a larger rearward shift than would be expected theoretically.

The nose-up pitching moment needed to trim about a c.g. position at $0{\cdot}35c$ is plotted against C_μ' in Fig. 4e, at constant wing incidence and zero tailplane lift. The trimming power of tailplane incidence is seen to be quite inadequate with a tailplane of conventional size and type, except at small values of C_μ'; there is a further slight deterioration as the tailplane height is decreased from $h = 1{\cdot}2c$ to $0{\cdot}3c$. The trimming power of a vertical round jet, directed upwards to produce negative lift at the tailplane quarter-chord is also indicated in Fig. 4e. For example, to trim a wing C_L of about 5 at $\alpha = 0$ ($C_\mu' = 1{\cdot}8$, $\eta = 60°$) with zero tailplane lift, a tail-jet momentum coefficient $C_{JT}(\equiv J_T/q_0 S)$ of around $0{\cdot}5$ would be needed, i.e. blowing with about one-quarter of the gross jet-flap wing momentum and a lift *loss* of some 10%. On these grounds, there seems much to commend the use of a B.L.C. or jet-flap tailplane for trimming to alleviate the auxiliary blowing requirements, or better still a foreplane to preclude lift loss with trimming.

3.4. *Thrust.*

The experimental thrust-lift curves are given in Fig. 5 at constant C_μ'-values and flap angles. For $\eta = 0°$ and 30°, the thrust remained positive at all incidences below the stall, provided C_μ'

---

* $\nu \simeq \dfrac{S'(\partial C_L/\partial\alpha)_\infty + (S-S')(\partial C_L/\partial\alpha)_\infty, C_\mu' = 0}{S(\partial C_L/\partial\alpha)_\infty}$.

† Again without transition wires on wing; the effect of adding transition wires on the pitching moment was to increase C_m by not more than $0{\cdot}06$.

exceeded about 0·1. For $\eta = 60°$, the thrust became positive only at negative incidences unless C_μ' was high ($> 2·3$), while for $\eta = 90°$ the thrust was never positive becoming more and more negative with increasing C_μ'.

To analyse the practical deficiency in thrust, relative to that expected from linearised inviscid-flow theory, an empirical sectional thrust coefficient $C_{T\infty}'$ may be conveniently defined by a relation of the type

$$\frac{S'}{S} C_{T\infty}' = C_T + C_{D0} + k \frac{C_L^2}{\pi A + 2C_\mu'}.$$

Here C_T signifies the measured thrust coefficient and C_{D0} the measured zero-lift drag ($C_\mu' = \eta = 0$); $kC_L^2/(\pi A + 2C_\mu')$ represents an allowance for the basic 'trailing-vortex' drag associated with finite aspect-ratio effects expressed as a factor k times the theoretical value for an elliptic loading[11], while S'/S is a part-span conversion factor to allow for the body cut-out.

The empirical values thus derived for $C_{T\infty}'$ are plotted in Fig. 5e against C_μ', for $\alpha = 0$ and $\eta = 0$, 30°, 60°, assuming that k is either 1·0 or 1·1. For flap angles up to 30°, $C_{T\infty}'$ remains sensibly proportional to C_μ' and independent of η. The ratio $C_{T\infty}'/C_\mu' \doteq 0·84$ is considerably less than the theoretical value of unity but practically the same as the static experimental value of 0·85 (*see* Section 2.3). For $\eta = 60°$ and C_μ'-values well above those needed solely for boundary-layer control, $C_{T\infty}'/C_\mu'$ falls to about 0·65 with $k = 1·0$ or only to 0·7 with $k = 1·1$. Analysis of the thrust results for $\eta = 90°$ was not attempted, since large areas of separated flow were present over the wing nose, even at zero incidence.

The thrust results discussed in this paper are of course mostly appropriate to conditions of low-speed flight at landing and take-off, the C_μ'-values and ratio of jet efflux velocity to mainstream velocity being in general much larger than envisaged for cruising-flight conditions. Even so, it is worth noting that the ratio $C_{T\infty}'/C_\mu'$ at small flap angles could probably be raised from the value 0·84 obtained here to as high as 0·92 by improved slot design and flap nose alignment (*see* Section 2.3). Again, if the flap were of a retractable type, providing a good trailing-edge slot configuration without jet deflection (for cruise), the value could rise to 0·97 under such conditions; practically the same as that for a conventional round nozzle*. Experimental results on such thrust aspects will be reported soon by Wood from his R.A.E. experiments[7,9].

3.5. *Part-Span Flaps.*

The entire wing of the aspect-ratio 6 model actually comprised two identical parts of equal spanwise extent with independent flaps. However, the presence of the body restricted the effective span of the inboard flap to 0·8 of that of the outer flap, the slot extent inside the body being permanently sealed (Fig. 1b)†. Some zero-incidence tests were made with the outboard flap undeflected and the inboard flap at 30° and 60°, both with full-span blowing and with blowing only over the inboard flap. For the discussion of part-span effects in this section and the next, the results are more usefully compared in terms of C_μ (based on gross wing area) rather than C_μ'.

Fig. 6a shows the lifting effectiveness of part-span flaps with full-span blowing. With the inboard flap alone deflected 60° ($\theta = 67°$), the lift nearly equalled that for a full-span flap deflection of 30°

* Practical full-scale jet-flap aircraft may well rely mainly on separate round jets for thrust, and also have the jet-flap nozzle inoperative in cruising flight.

† The term full-span blowing is used here for convenience, even though the body cut-out is present.

($\theta = 37°$) at the same C_μ. Likewise, with the inboard flap alone deflected 30° ($\theta = 37°$), the lift was roughly midway between that for full-span flaps at $\eta = 0°$ and 30° ($\theta = 7°$ and 37°). Thus, with full-span blowing, the lift was roughly proportional to the flap span and jet deflection.

However, Fig. 7a shows that the thrust obtained with part-span flaps and full-span blowing was lower than that for full-span flaps set to yield the same lift coefficient at the same C_μ-value. For example, the reduction in C_T for $C_\mu = 2{\cdot}5$ and $C_L = 3$ was as much as 0·6!

Some extra zero-incidence tests were also made with the blowing (as well as deflection) limited to the spanwise extent of the inboard flaps, and the results are compared with those for full-span flap deflection and blowing in Figs. 6b and 7b. The flap angle required to achieve a prescribed C_L was somewhat less than twice the flap angle for full-span flaps and blowing at the same C_μ-value.

A tentative method of analysis for part-span flap effects is given in Ref. 9. However, there is as yet no adequate theoretical basis taking into account the spanwise variation of the height and inclination of the jet sheet relative to the datum wing chord plane as well as the modified spanwise distribution of lift loading and jet momentum.

3.6. *Effect of Slot Blockage (Part-Span Blowing).*

In order to assess the effectiveness of part-span blowing, such as might arise with a partial power failure in practice, some zero-incidence tests were made with various spanwise extents of the slot blocked and full-span flap deflections of 30° and 60°. For this purpose, the spanwise length of the slot from the wing-body junction to the wing tip was divided into equal quarters, the four possible combinations of any two of these blocked off at a time being investigated. The lifting effectiveness for the various distributions of overall momentum are compared in Fig. 6c, by plotting C_L against C_μ. The corresponding C_T vs. C_μ curves are given in Figs. 7c to 7f.

Liftwise, full-span blowing, with the slot completely open apart from the normal spacers, provided the most efficient usage of a given momentum at any fixed flap angle. The best partially blocked configuration occurred with the inboard half of the full-span slot open, but produced only about three-quarters of the lift for the fully open slot at the same C_μ and η (Fig. 6c). From comparison with the other configurations, blockage of the slot close to the root seemed particularly detrimental. Tuft studies confirmed that the loss in lift due to slot blockage was directly associated with changes in the spanwise loading distribution. Strong trailing vortices were observed at the edges of the broken jet sheet, and the 'blown' parts of the wing seemed to have little influence on the neighbouring unblown parts.

The thrust achieved at a prescribed C_L-value was considerably less with part-span blowing than with full-span blowing at the same C_μ, partly because of the higher jet deflection angle required and partly because of the extra pressure drag associated with the severe modifications to the spanwise loading distribution. Correspondingly, although the thrust measured with part-span blowing exceeded that for full-span blowing at the same η, the excess C_T was much less than the additional C_μ required to ensure the prescribed C_L-value.

3.7. *Effect of Flap-Nose Misalignment on Lifting Effectiveness.*

In the main series of tests, the upper surface of the flap nose was aligned so that it protruded into the middle of the jet. Additional tests were carried out, for $\alpha = 0°$ and $\eta = 60°$, with the flap lowered relative to the slot (width 0·08 in.) by amounts up to 0·5 in. Provided the gap between the wing and the flap was kept sealed on the underside, to prevent flow from the lower to the upper surface, the

jet turned and followed the upper surface of the flap without difficulty. A small vortex appeared to act as a 'roller-bearing' between the lower surface of the jet and the adjacent solid surface in the gap. When the flap was dropped 0·1 in. from its standard position, C_L fell by about 0·2 for $C_\mu' = 0{\cdot}1$, but the fall was negligible for C_μ'-values above unity. With the flap dropped 0·5 in., the loss remained roughly at 0·3 throughout the practical C_μ' range (*see* Fig. 8a). During tests with the gap unsealed, the jet did not follow the upper surface of the flap and there was a large loss in lift.

The results obtained for $\alpha = \eta = 0$ with the gap sealed are also worth mention. The lift coefficient *increased* slightly as the flap was lowered more than 0·05 in. probably due to an increase in the effective jet angle. The gain in C_L at prescribed C_μ' was about 0·2 with the flap 0·5 in. below the standard position; but, for the same C_L-value, the thrust coefficient was then much reduced (Fig. 8b).

3.8. *Downwash Investigations.*

Balance measurements were made on the model with a tailplane of variable height fitted ($l/c = 3{\cdot}1$), as described in Section 2.1, for ranges of wing incidence α (below the stall) and of relative tailplane angle α_T. Conventional tunnel corrections (*see* Section 2.2) were applied to the measured values. Some typical lift, pitching-moment and thrust results are given in Figs. 9, 10 and 11 respectively for the single case $h/c = 1{\cdot}2$, $\eta = 60°$. The pitching-moment curves were used to derive the mean downwash ϵ over the tailplane, by standard methods[15].

Curves of ϵ vs. α, plotted at constant C_μ'-values, are given in Fig. 12, for $h/c = 1{\cdot}2$ with $\eta = 30°$ and 60°, and for $h/c = 1{\cdot}2$, 0·9, 0·3 with $\eta = 60°$. Fig. 13 shows cross-plots of ϵ vs. η with $\alpha = 0°$ and $h/c = 1{\cdot}2$, and of ϵ vs. h/c with $\alpha = 0°$ and $\eta = 60°$.

As might be expected, the combination of high lift and large jet deflection produced values of downwash much greater than those normally encountered. For example, with $\alpha = 0°$ and $\eta = 60°$, the value of ϵ at $h/c = 1{\cdot}2$ rose steadily from about 3° to 15° as C_μ' was increased from 0 to 2·4, while $(1 - \partial\epsilon/\partial\alpha)$ fell from about 0·7 to 0·5. Furthermore, if h/c was reduced to 0·3 at $C_\mu' = 2{\cdot}4$, then ϵ rose about another 4°.

Some theoretical estimates, based on the work of Ross[13] with modifications to allow for trailing-edge-flap chord and aerofoil thickness, are included in Fig. 13 for C_μ'-values ranging from 0·7 to 8. Although the theoretical variation of ϵ with h/c at fixed C_μ', θ and α is plausible, the absolute values are far too low at high C_μ'. This could well be due to theory overestimating the variation, with C_μ', α or θ, of the effective distance of the deflected jet sheet below the tailplane. Moreover, the present theory ignores the rolling-up of the trailing-vortex sheet and deviations from the assumed elliptic spanwise loading distribution across the wing and the jet.

4. *Conclusions.*

The present balance measurements have confirmed the significant magnification of the direct jet-reaction lift, by the generation of wing pressure lift, found in the early pressure-plotting experiments on small-scale models[2,3]. The centre of lift and aerodynamic centre both moved rearward appreciably with increasing C_μ'. Although the stalling angle of the 12% thick wing tended to fall with increasing flap deflection at small C_μ'-values, due to precipitation of flow separation over the wing nose, there was a recovery of stalling angle at large C_μ' since the jet then induced re-attachment forward of the slot exit. In practice, such flow separations could profitably be minimised by wing nose B.L.C.[4,9].

The sectional thrust coefficient for the model, derived by making a theoretical allowance for the 'trailing-vortex' drag, falls significantly below the ideal-value C_μ', especially when the flap angle is above 30°. The origin of the deficiencies at small flap angles has now been clarified and some improvements have proved feasible by improved slot design and flap-nose alignment. Furthermore, for cruising conditions, the thrust attainable with the flap retracted fully, to provide a good wing trailing-edge slot, should compare favourably with that from a conventional nozzle. For a proper analysis of thrust at large flap angles, some comprehensive *two-dimensional* experiments are needed, including accurate balance measurements, pressure-plotting and flow studies.

The trimming power of a conventional tailplane is likely to be totally inadequate for practical c.g. positions, but the addition of auxiliary trimming jets at the tail or of blowing over the tailplane itself (B.L.C. or jet flap) could suffice. Even so, the trimming losses on lift would be appreciable and $d\epsilon/d\alpha$ would vary significantly with C_μ', so that a foreplane layout is naturally worth consideration.

Satisfactory predictions of lift are possible by simple modifications to inviscid-linearised-flow theory, at least with full-span flaps and blowing, provided there is little flow separation over the wing nose. However, as yet, reliable estimates of thrust and downwash, or of the influence of part-span flaps and blowing, can be ensured only by the introduction of empirical arguments and parameters. There is clearly need for further theoretical and experimental research on such aspects, particularly as regards the effects arising from viscous flows and the substantial divergence of the trailing jet sheet from the wing chord plane.

Acknowledgements.

Miss E. M. Love and Miss L. M. Esson assisted with the experiments and reduction of observations at N.P.L. The model was designed by Mr. N. Marcus, being constructed partly by N.P.L. Aerodynamics Workshop and partly by Hunting Aircraft Ltd.

LIST OF SYMBOLS

A_t	Slot throat area
c	Wing chord = 1·6 ft
c_f	Flap chord aft of hinge-line = 0·16 ft
C_L	Lift coefficient = (measured lift)/$q_0 S$
ΔC_L	Increment in lift coefficient due to flap deflection and blowing
$\frac{\partial C_L}{\partial \alpha}, \frac{\Delta C_L}{\Delta \alpha}$	Lift-incidence curve slopes, theoretical and experimental
$\frac{\partial C_L}{\partial \theta}$	Theoretical rate of variation of lift coefficient with jet deflection
C_m	Pitching-moment coefficient about 35% chord = (measured moment/$q_0\ Sc - 0{\cdot}57(\partial C_m/\partial_T \alpha)C_L$ tail on
C_T	Thrust coefficient = (measured thrust)/$q_0\ S - 0{\cdot}0105 C_L{}^2$
C_{D0}	Drag coefficient at zero lift without flap deflection or blowing
$C_\mu{}', C_\mu$	Sectional and overall blowing momentum coefficients = $M_J V_J/q_0 S'$, $M_J V_J/q_0 S$,
F	Aspect-ratio conversion factor on lift
h	Height of tailplane above fuselage centre-line
J	Static jet reaction
k	Basic 'trailing-vortex' drag factor
l	Distance of tailplane quarter-chord aft of wing quarter-chord = 5·125 ft
M_J	Rate of mass flow (slugs/sec) of air to model
p_D	Total pressure in slot throat (lb/sq. ft)
p	Mainstream static pressure
q_0	Mainstream dynamic head
S	Gross wing area = 8·33 sq. ft
S'	Reference wing area corresponding to spanwise extent of blowing slot = 7·50 sq. ft for full-span blowing
V_0	Mainstream speed
V_J	Jet speed evaluated theoretically by assuming isentropic expansion from mean total pressure in slot throat to mainstream static pressure
α	Wing incidence = (geometrical incidence) + 0·60 C_L degrees
α_T	Angle of tailplane relative to fuselage centre-line
$\Delta\alpha_T$	Increment of tailplane angle relative to zero-lift position
ϵ	Mean downwash at tailplane relative to fuselage centre-line = (measured downwash) + 1·17C_L degrees
η	Flap angle
θ	Effective jet angle

Suffix ∞ implies that value is appropriate to two-dimensional conditions.

REFERENCES

No.	Author(s)	Title, etc.
1	I. M. Davidson	The jet flap. *J. R. Aero..Soc.*, Vol. 60, pp. 25 to 50. 1956.
2	N. A. Dimmock	Some early jet-flap experiments. *Aero. Quart.*, Vol. 8, pp. 331 to 345. 1957.
3	J. Williams and A. J. Alexander ..	Some exploratory three-dimensional jet-flap experiments. *Aero. Quart.*, Vol. 8, pp. 21 to 30. 1957.
4	J. Williams and E. M. Love ..	Simple jet-flap experiments comparing blowing from the trailing-edge, from the knee of a trailing-edge flap, and from the aerofoil nose. Unpublished N.P.L. paper.
5	J. Williams	British research on the jet-flap scheme. *Z.F.W.* (Germany), Vol. 6, pp. 170 to 176. 1958.
6	A. J. Alexander and J. Williams ..	Interim note on wind-tunnel experiments on a rectangular-wing jet-flap model of aspect-ratio 6. A.R.C. 19,888. February, 1958.
7	M. N. Wood	Further wind-tunnel experiments on a rectangular-wing jet-flap model of aspect-ratio 6. A.R.C. 21,866. September, 1959.
8	S. F. J. Butler, M. B. Guyett and B. A. Moy	Six-component low-speed tunnel tests of jet-flap complete models with variation of aspect ratio, dihedral and sweepback, including the influence of ground proximity. Unpublished M.o.A. Report.
9	J. Williams, S. F. J. Butler and M. N. Wood	The aerodynamics of jet flaps. A.R.C. R. & M. 3304. January, 1961.
10	D. A. Spence	The lift on a thin aerofoil with a jet-augmented flap. *Aero. Quart.*, Vol. 9, pp. 287 to 299. 1958.
11	E. C. Maskell and D. A. Spence ..	A theory of the jet-flap in three dimensions. *Proc. Roy. Soc.* A., Vol. 251, pp. 407 to 425. 1959.
12	E. C. Maskell	The interference on a three-dimensional jet-flap wing in a closed wind tunnel. A.R.C. R. & M. 3219. August, 1959.
13	A. J. Ross	The theoretical evaluation of the downwash behind jet-flapped wings. A.R.C. R. & M. 3119. January, 1958.
14	A. Anscombe and J. Williams ..	Some comments on high-lift testing in wind-tunnels with particular reference to jet-blowing models. *J. R. Aero. Soc.*, Vol. 61, pp. 529 to 540. 1957.
15	S. F. J. Butler and J. Williams ..	Further comments on high-lift testing in wind-tunnels with particular reference to jet-blowing models. *Aero. Quart.*, Vol. XI, pp. 285 to 308. 1960.
16	R. C. Pankhurst and D. W. Holder	*Wind-tunnel technique.* Pitmans, London. 1952.

APPENDIX

Tunnel-Speed and Tare-Force Calibrations

The false wall reflection-plane was 16 ft long, spanning the 13 ft × 9 ft Tunnel vertically (i.e. 9 ft high), but was fixed well to one side laterally in the tunnel—roughly 3·5 ft from the nearest tunnel wall. The main feed pipes, air-bearing connector and bracing struts formed a large solid blockage between the side of the false wall remote from the model and the adjacent tunnel wall. As expected, this caused an appreciable velocity difference between the two sides of the false wall but, provided the flow past the model in the modified working section remained sensibly uniform, this was not objectionable. To provide some control on the flow distribution, the false wall was fitted with L.E. and T.E. flaps each of 1 ft chord and variable setting. Comprehensive static-pressure and speed explorations were then completed with the model and blowing rig in position, as any gradient could be especially significant in the tail-on tests.

First, static-pressure distributions were measured down the length of the wall, both above and below the model centre-line, with the model in its datum attitude ($\alpha = \eta = C_{\mu}' = 0$). It was shown that, as regards minimum static-pressure gradient, the L.E. flap was best left undeflected but the T.E. flap was best deflected about 4° towards the model side. Typically, the static-pressure changes, for streamwise locations between the wing and tailplane positions, were then less than $\pm\frac{1}{2}\%$ of the mainstream dynamic head, except of course close to the body. Pitot-static traverses were also made along wind, at distances $\frac{1}{2}$ ft and 2 ft out from the false wall some 2 ft above and below the model centre-line. These indicated a random velocity variation of less than $\pm 1\%$ across the new working section, and a slight steady rise in velocity downstream of the wing of less than 1%. A few similar traverses between the false wall and the tunnel wall gave velocities only about 90% ($\pm 1\%$) of those in the new working section on the model side of the false wall.

Naturally, the effects of incidence, flap deflection, and blowing were considerable in the vicinity of the wing, due to the development of circulation lift. However, the local mainstream speed at the nose and tail of the model rose by only about 1%, when the nominal tunnel speed as given by the difference between statics at the beginning and end of the tunnel contraction was maintained constant.

In this particular blowing-model rig, the weight and airloads from the floating link of the air-bearing connector and the associated feed pipes to the model were supported on the main balance, so these were measured simultaneously with the forces and moments on the model proper. In order to evaluate the corrections for such tare forces, balance measurements of lift, pitching moment and thrust were made over a range of incidence and flap deflections (without blowing), first for the complete model rig, and then after disconnection of the airbearing link and feed pipes from the balance. The tare corrections thus derived were in fact relatively small, being about 1 lb lift, 2 lb thrust, and $\frac{1}{2}$ lb. ft pitching moment at a windspeed of 100 ft/sec, so that $\Delta C_L \simeq 0{\cdot}01$, $\Delta C_T \simeq 0{\cdot}02$, $\Delta C_m \simeq 0{\cdot}003$; these corrections were practically independent of incidence and flap angle up to the stall. As it was not possible to seal off the jet-flap blowing slot completely, the duct was sealed to ascertain the tare effects of pressurising the air-bearing and feed pipes. The lift increased by as much as 0·5 lb, but the thrust and moment increases were less than 0·05 lb and 0·1 lb. ft respectively, so that at 100 ft/sec these tare corrections were $\Delta C_L \simeq -0{\cdot}005$, $\Delta C_T \simeq -0{\cdot}0005$, $\Delta C_m \simeq -0{\cdot}0006$.

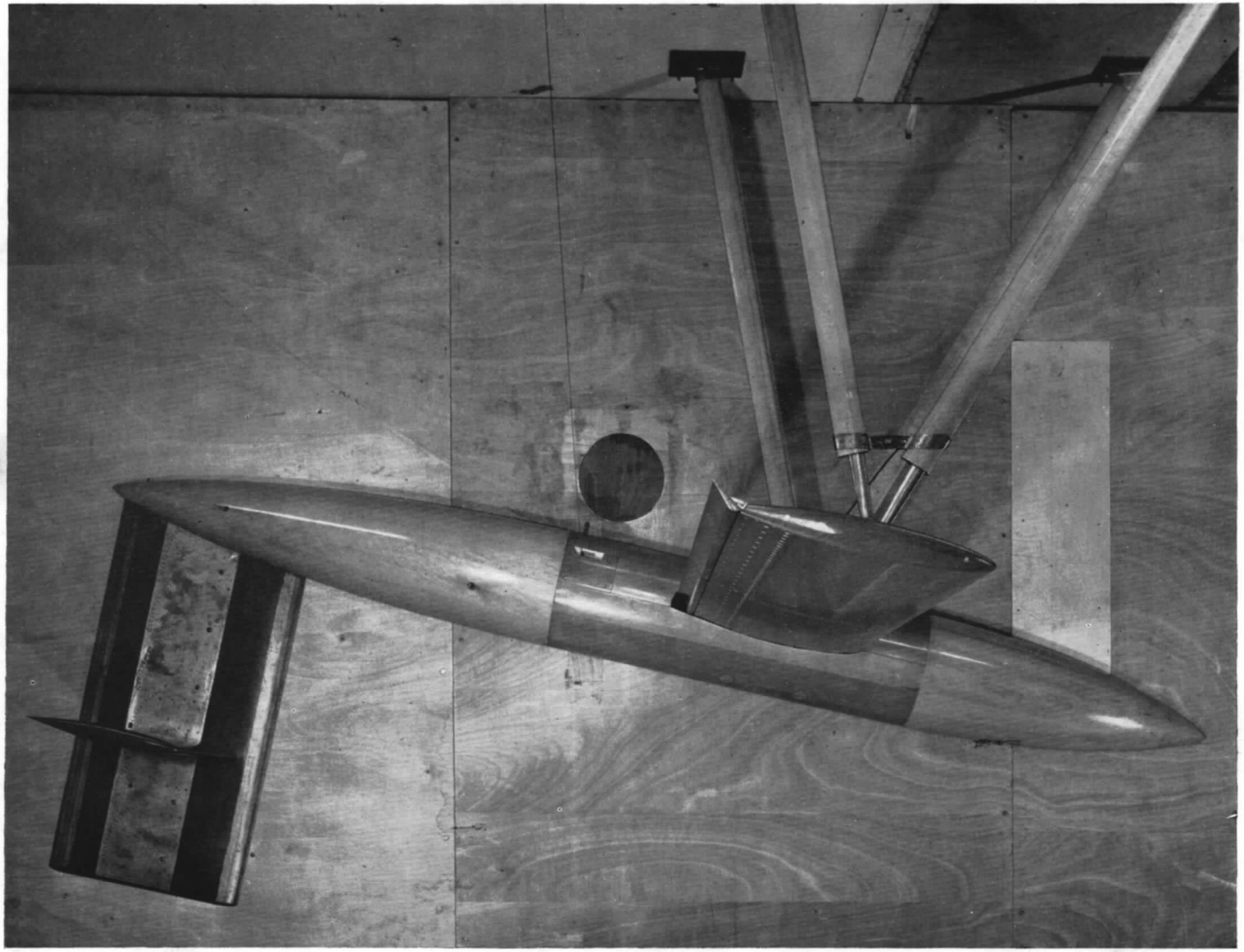

FIG. 1a. Half-model hung in 13 ft × 9 ft Tunnel from overhead balance.

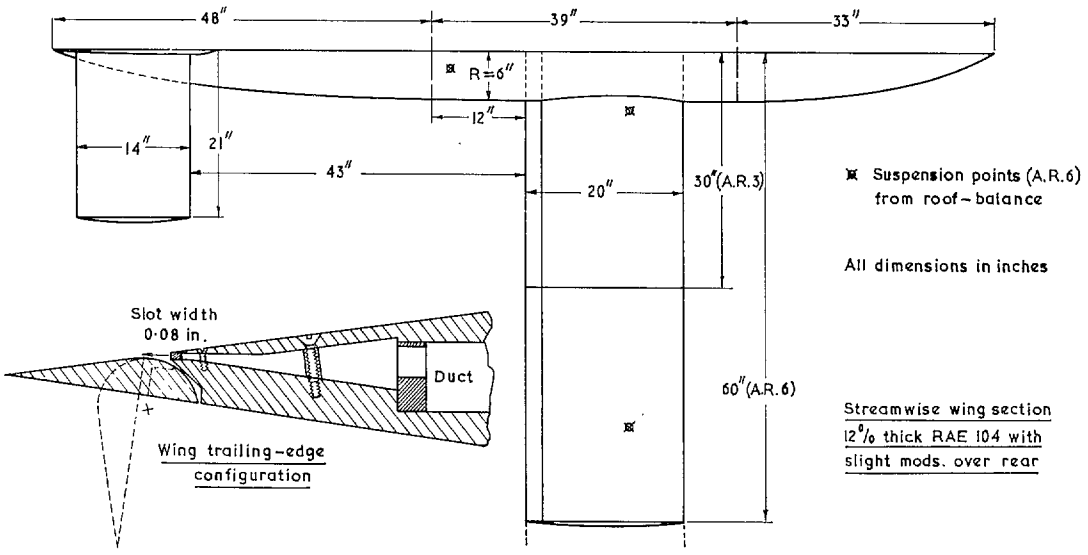

FIG. 1b. Rectangular-wing jet-flap half-model.

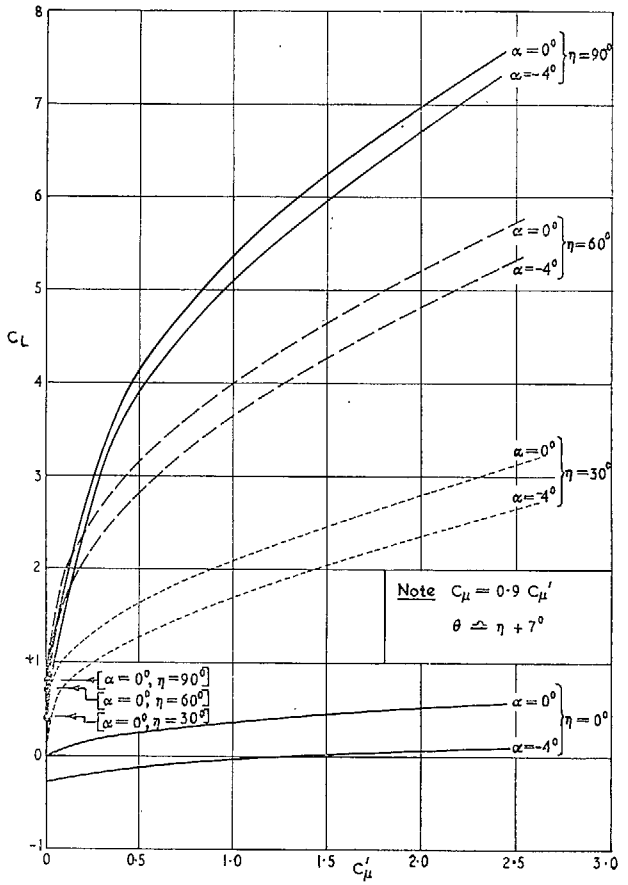

FIG. 2a. Variation of lift with momentum coefficient at constant incidence and flap angle.

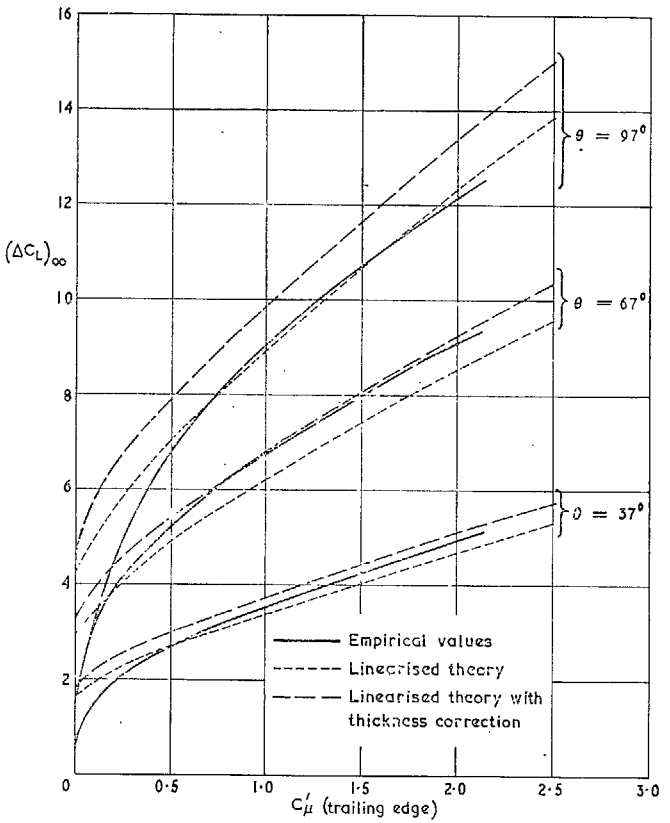

FIG. 2b. Comparison of 'two-dimensional' empirical and theoretical values for lift increment at zero incidence.

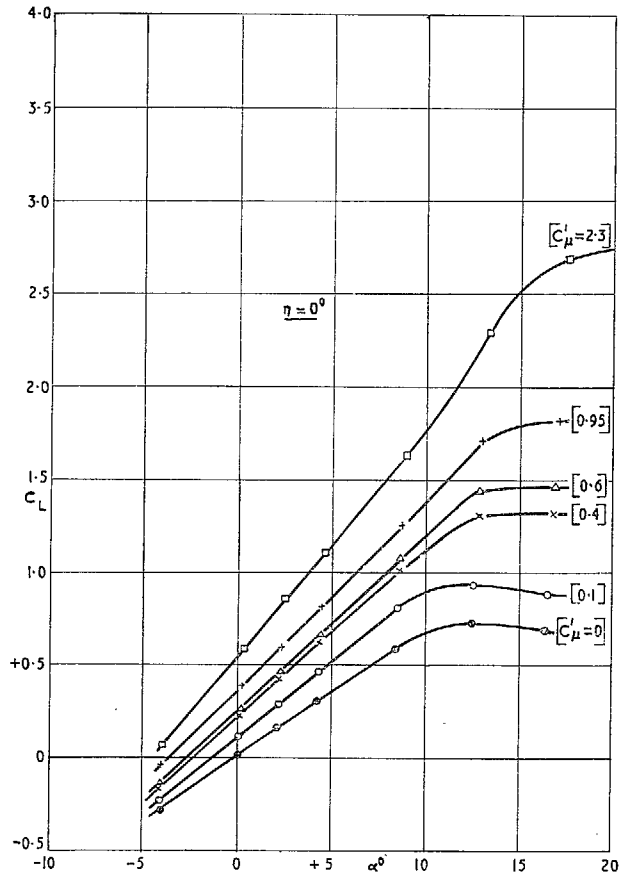

FIG. 3a. Variation of lift with incidence at constant C_μ', for $\eta = 0°$.

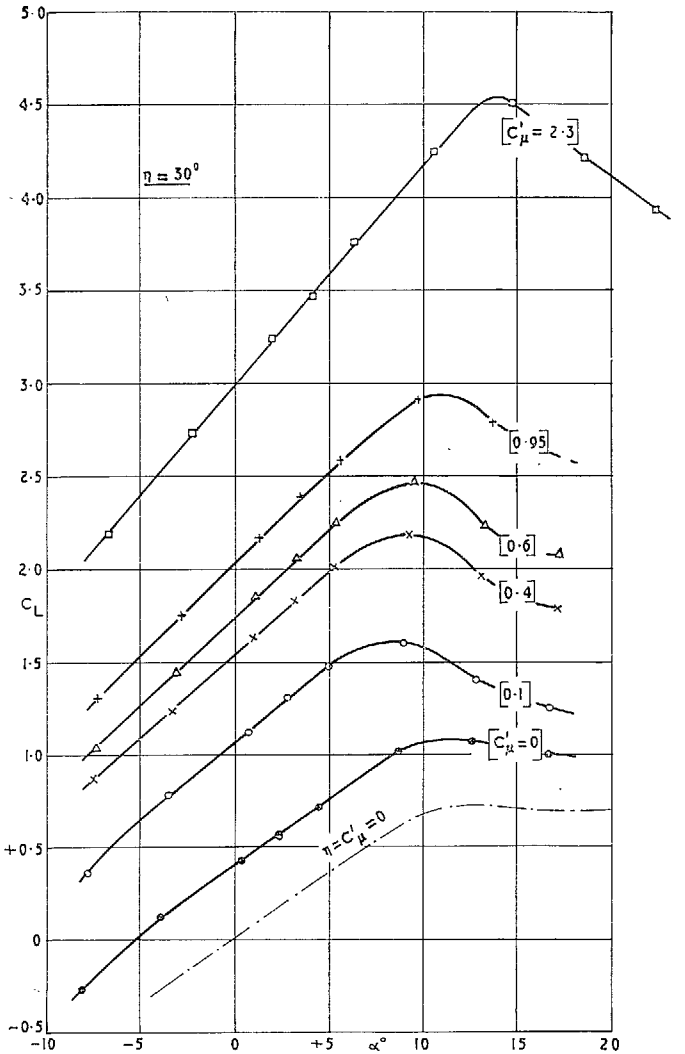

FIG. 3b. Variation of lift with incidence at constant C_μ', for $\eta = 30°$.

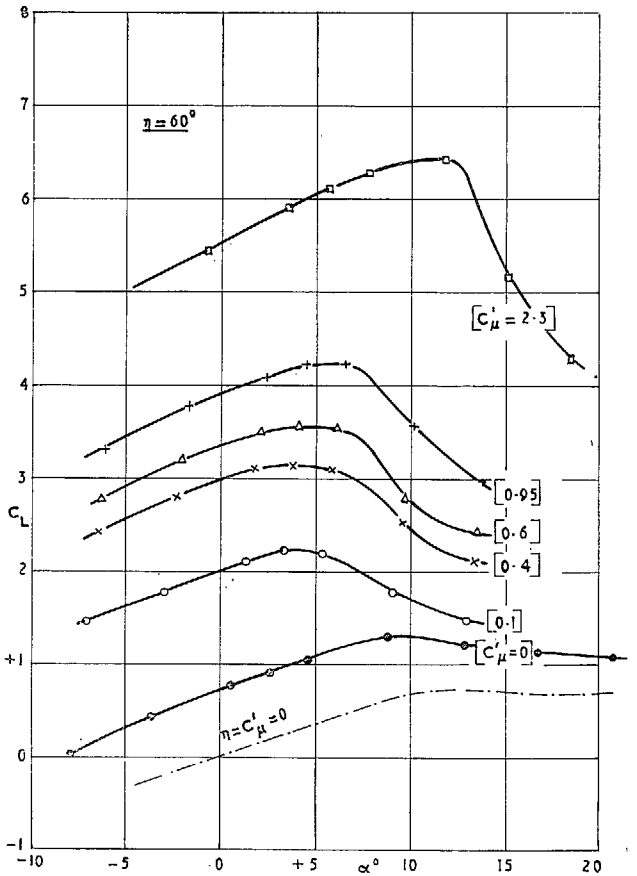

FIG. 3c. Variation of lift with incidence at constant C_μ', for $\eta = 60°$.

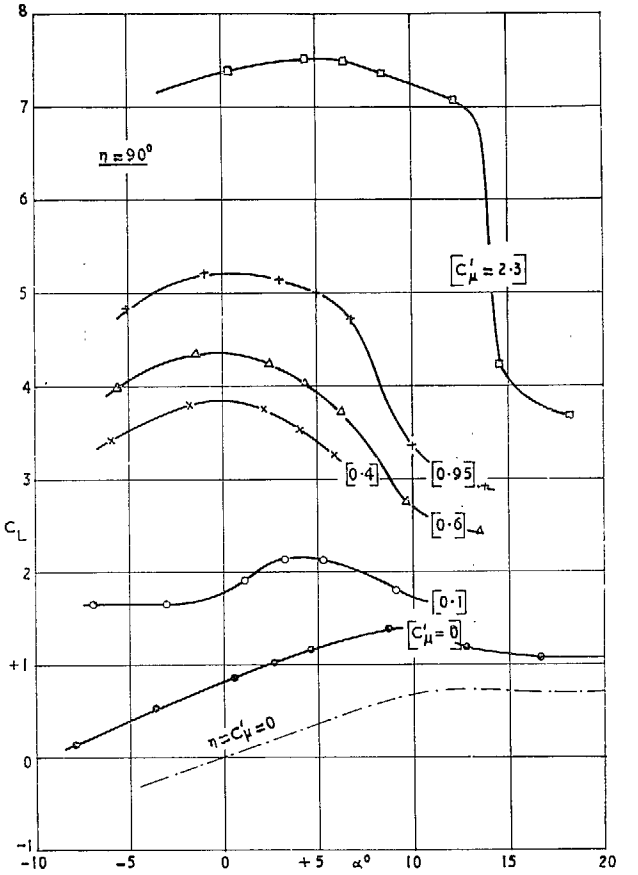

FIG. 3d. Variation of lift with incidence at constant C_μ', for $\eta = 90°$.

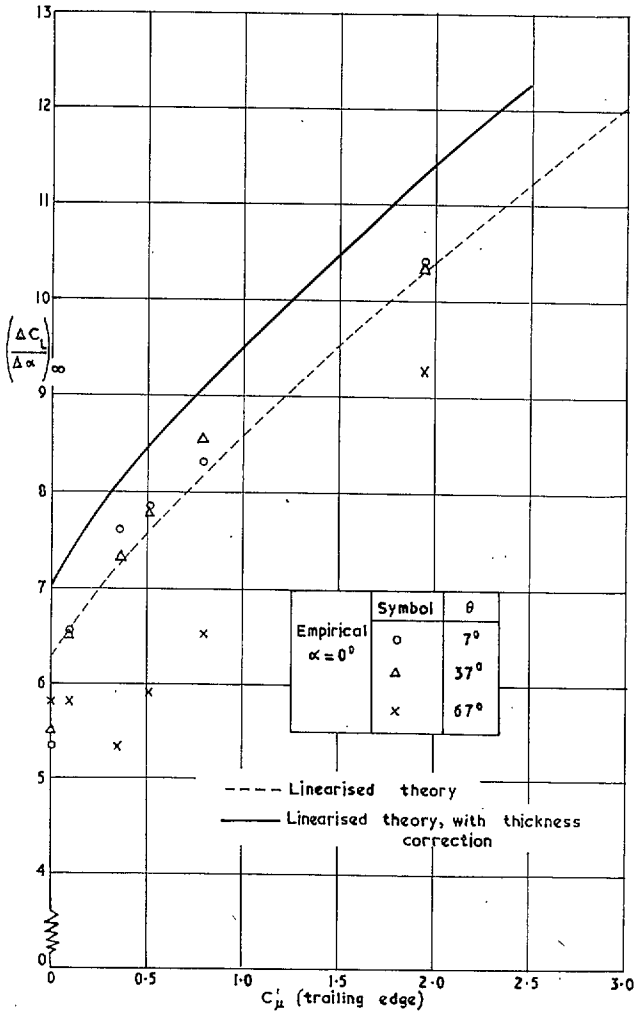

FIG. 3e. Comparison of 'two-dimensional' empirical and theoretical values for lift-incidence curve slope.

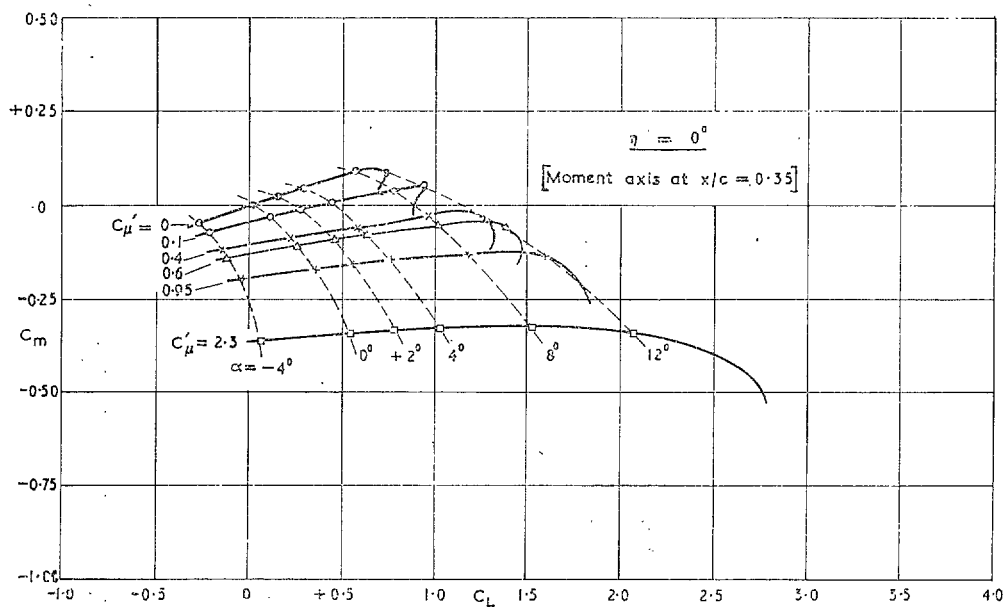

FIG. 4a. Variation of pitching moment with lift, for $\eta = 0°$.

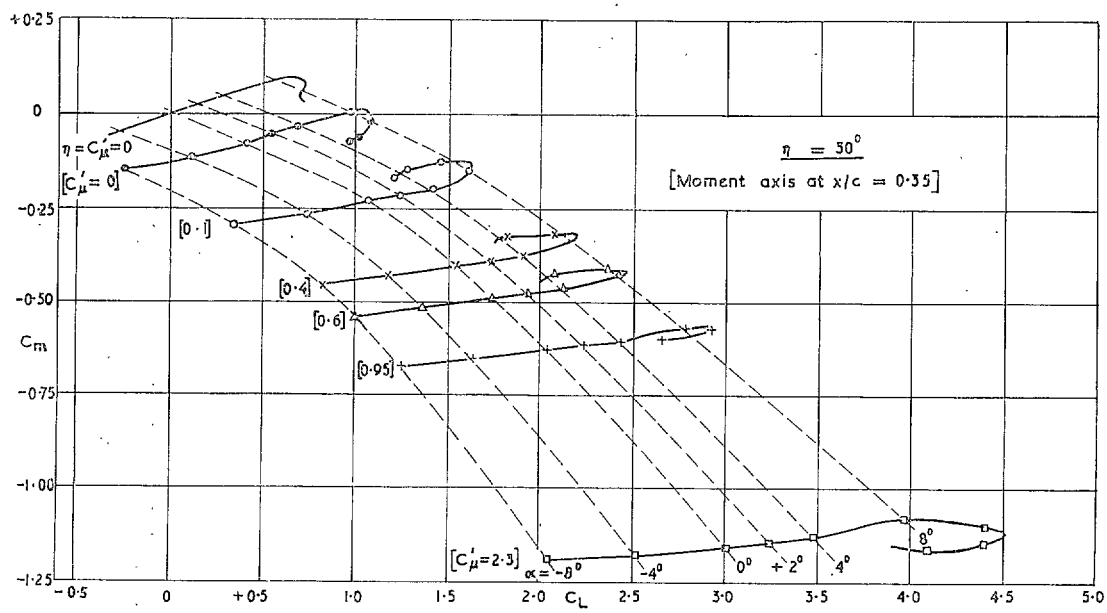

FIG. 4b. Variation of pitching moment with lift, for $\eta = 30°$.

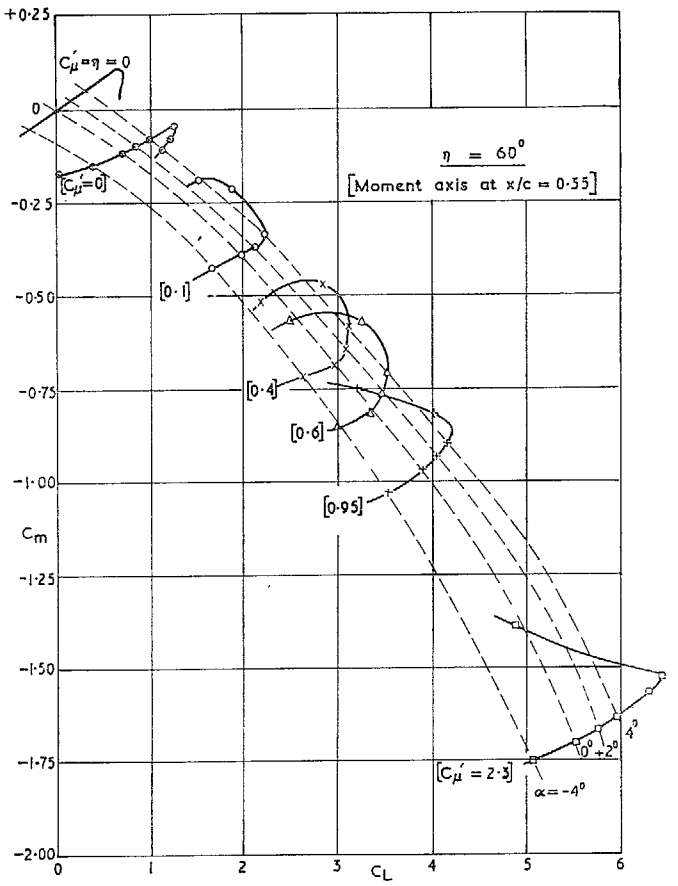

FIG. 4c. Variation of pitching moment with lift, for $\eta = 60°$.

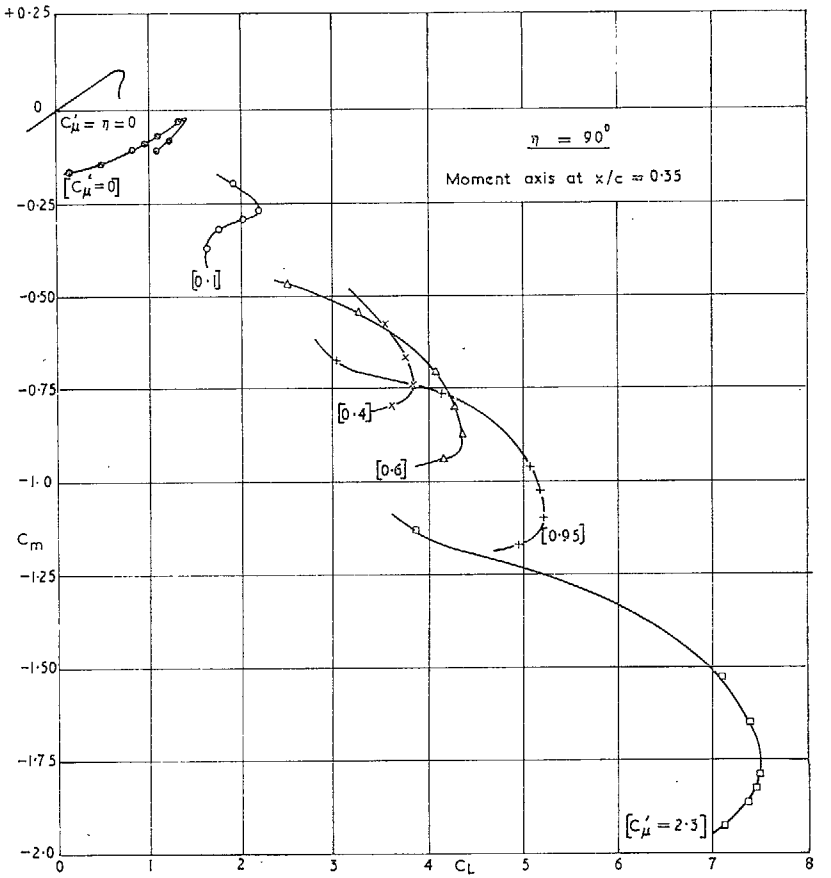

FIG. 4d. Variation of pitching moment with lift, for $\eta = 90°$.

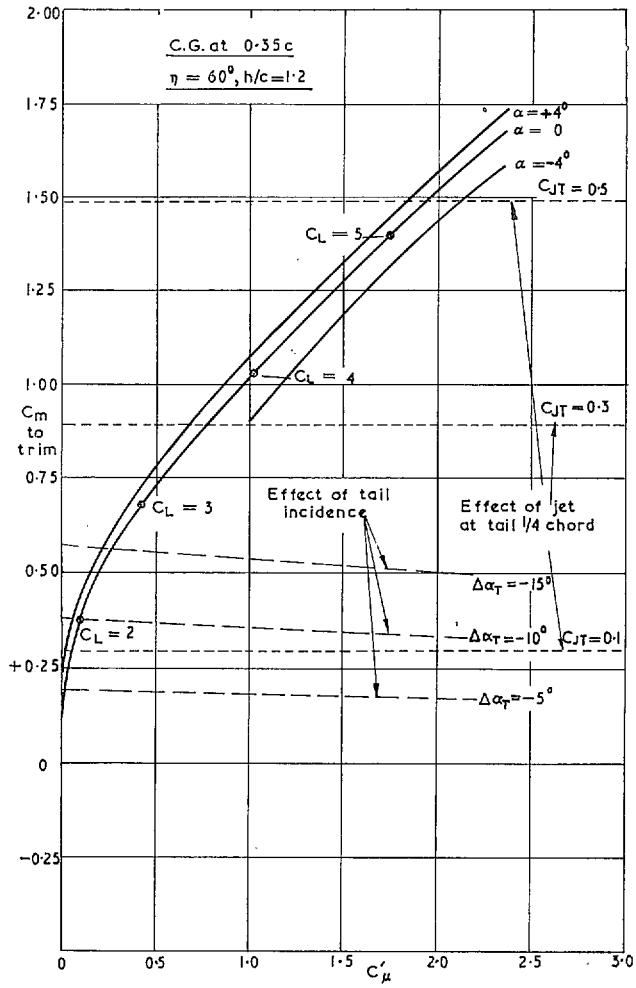

FIG. 4e. Pitching moment to trim with zero tail-plane lift.

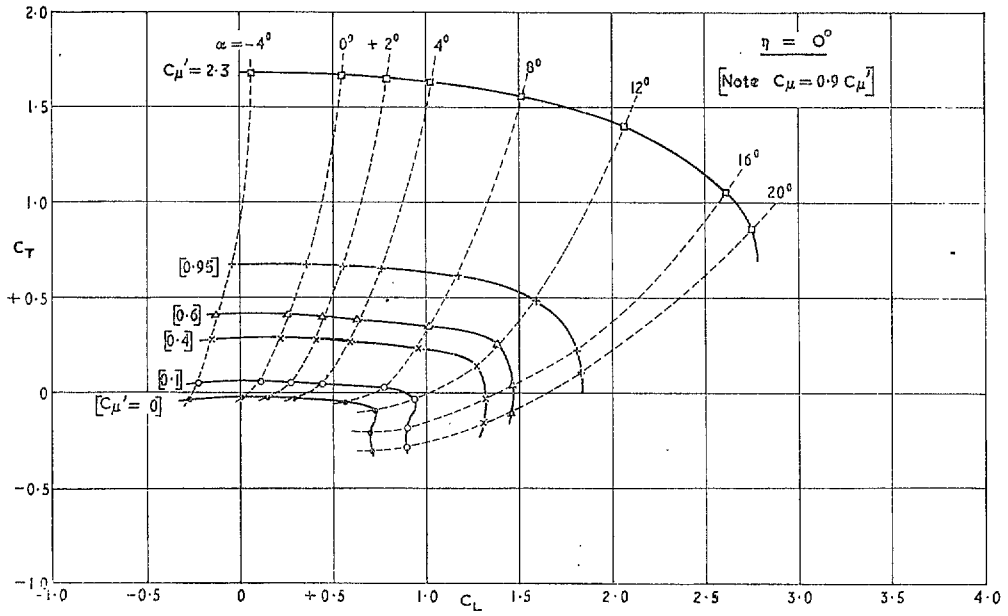

FIG. 5a. Variation of thrust with lift, for $\eta = 0°$.

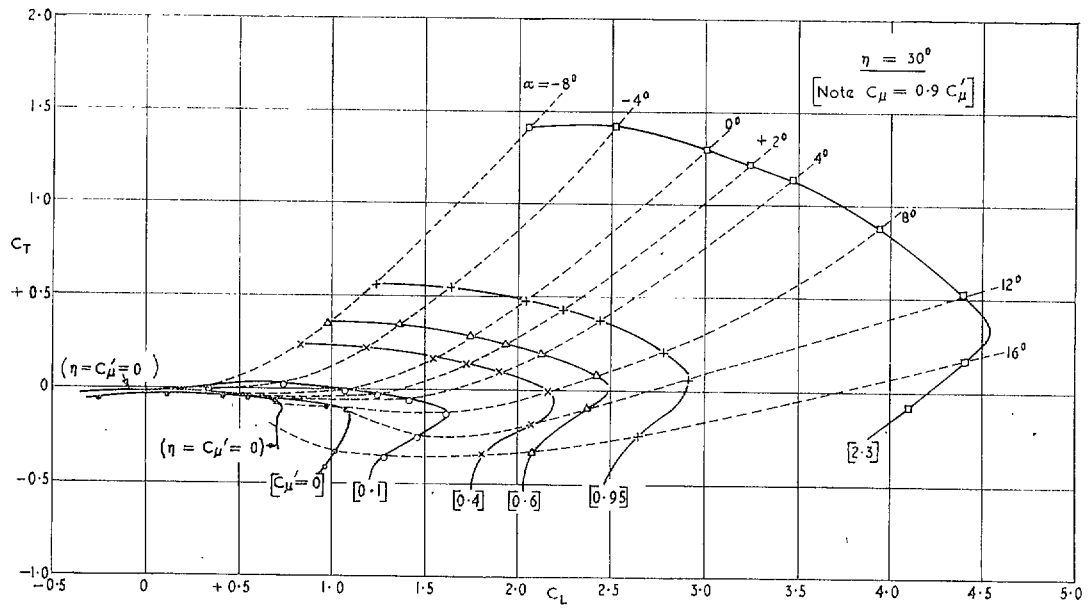

FIG. 5b. Variation of thrust with lift, for $\eta = 30°$.

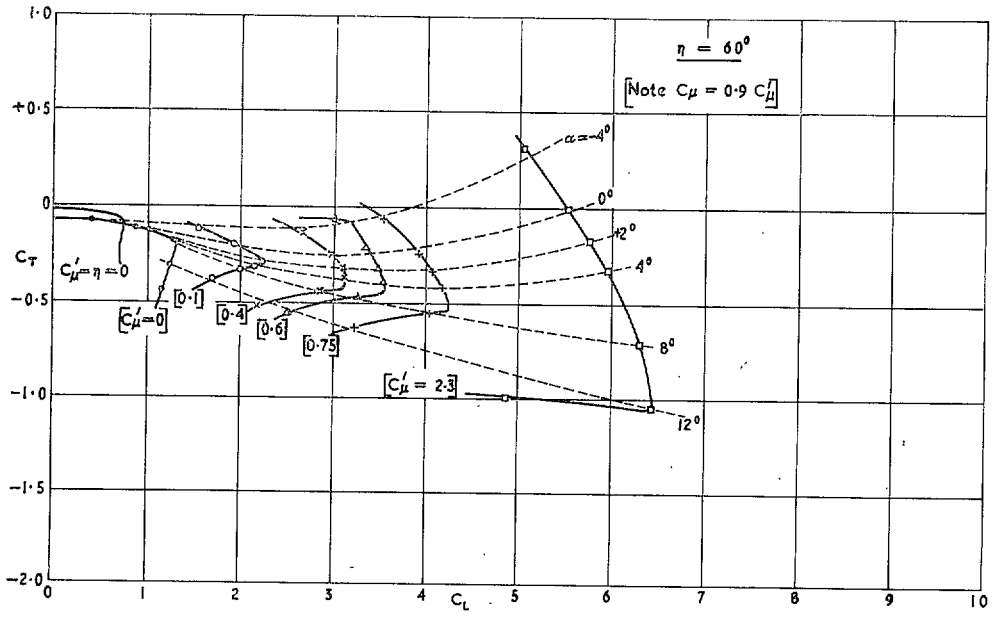

FIG. 5c. Variation of thrust with lift, for $\eta = 60°$.

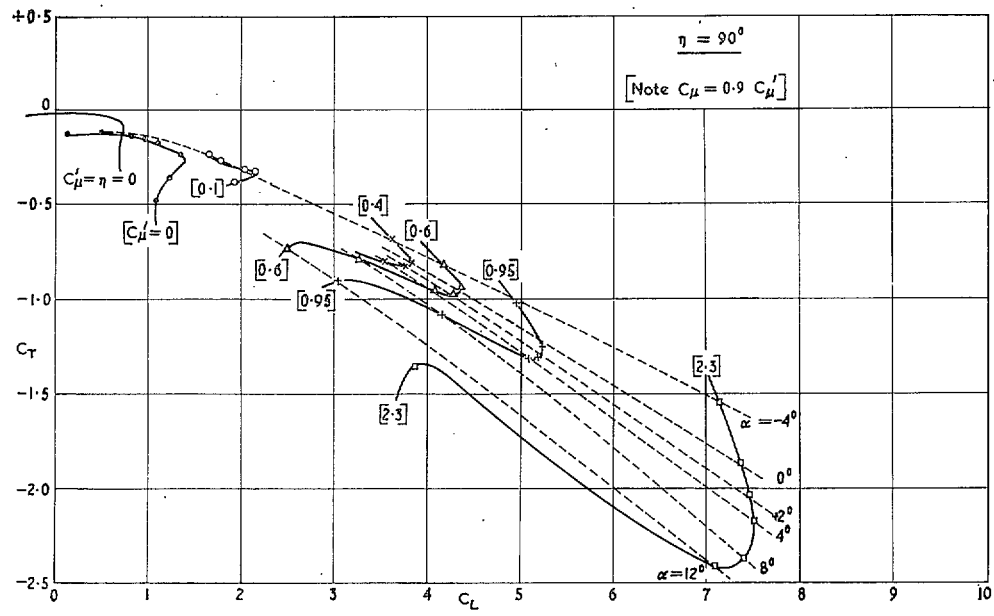

FIG. 5d. Variation of thrust with lift, for $\eta = 90°$.

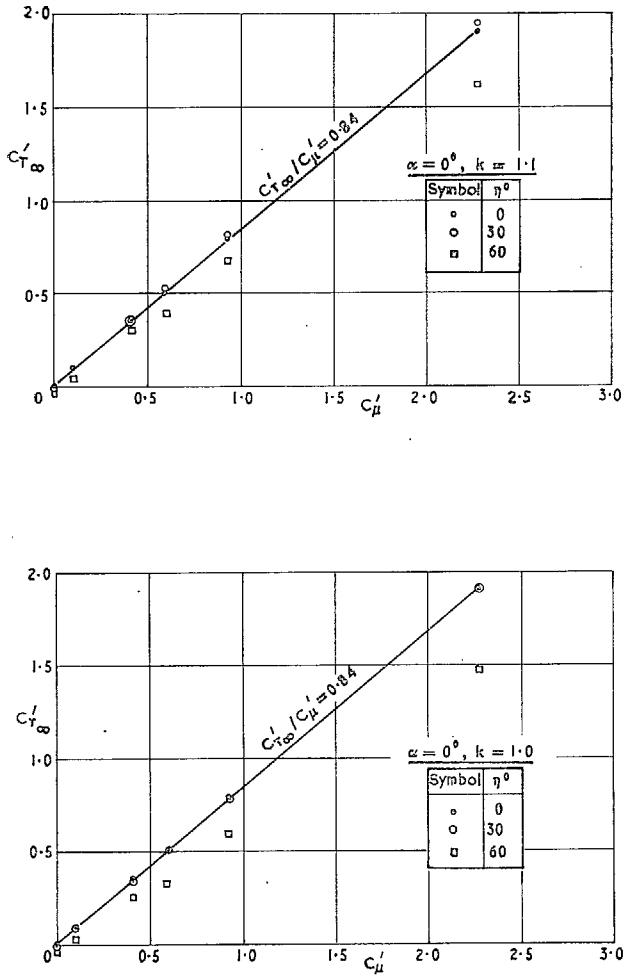

FIG. 5e. Variation of empirical sectional thrust with C_μ'.

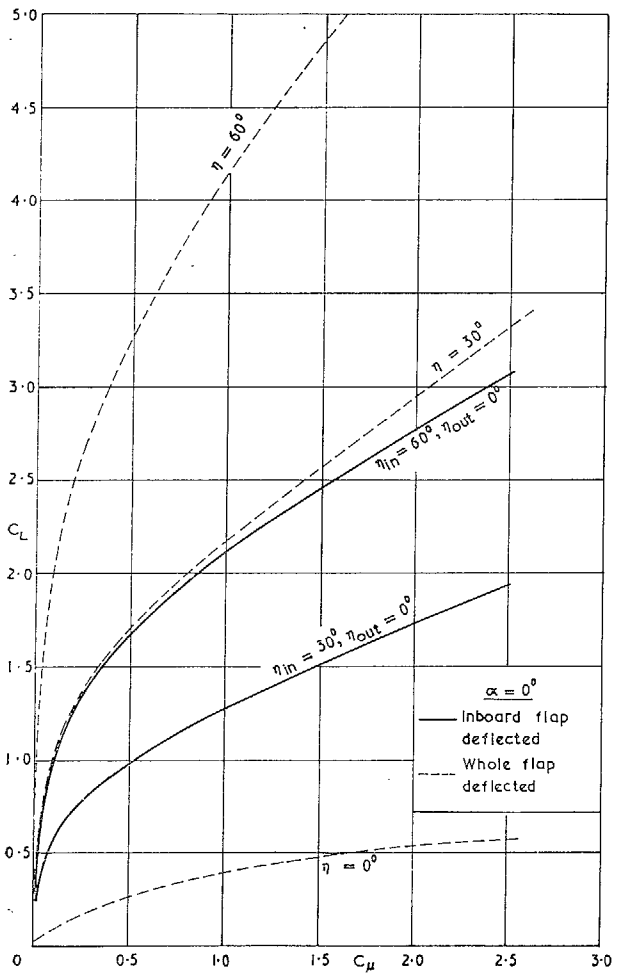

FIG. 6a. Lift for part-span flap with full-span blowing; $\alpha = 0°$.

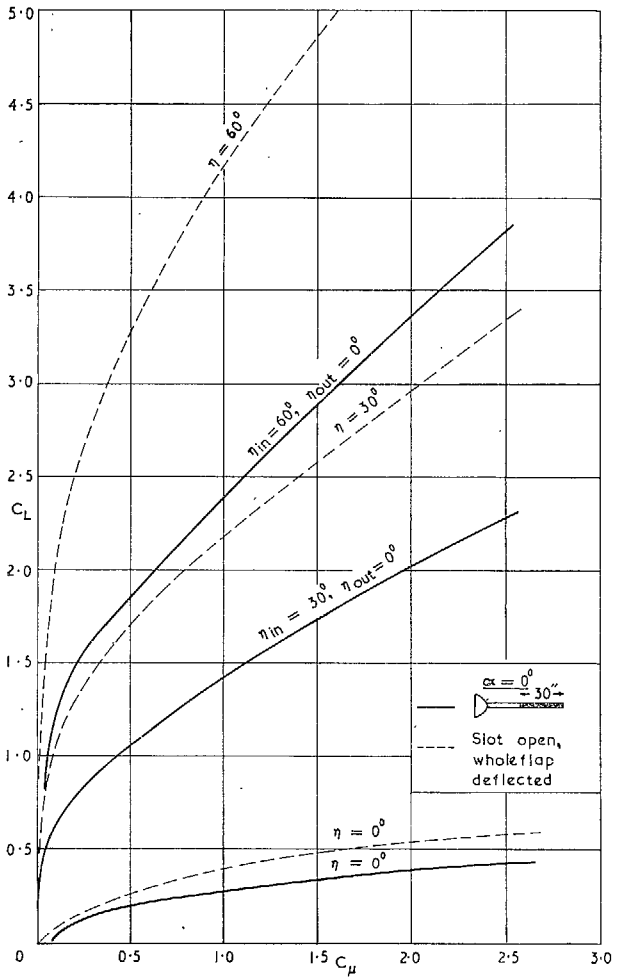

FIG. 6b. Lift for blowing over inboard deflected flap only; $\alpha = 0°$.

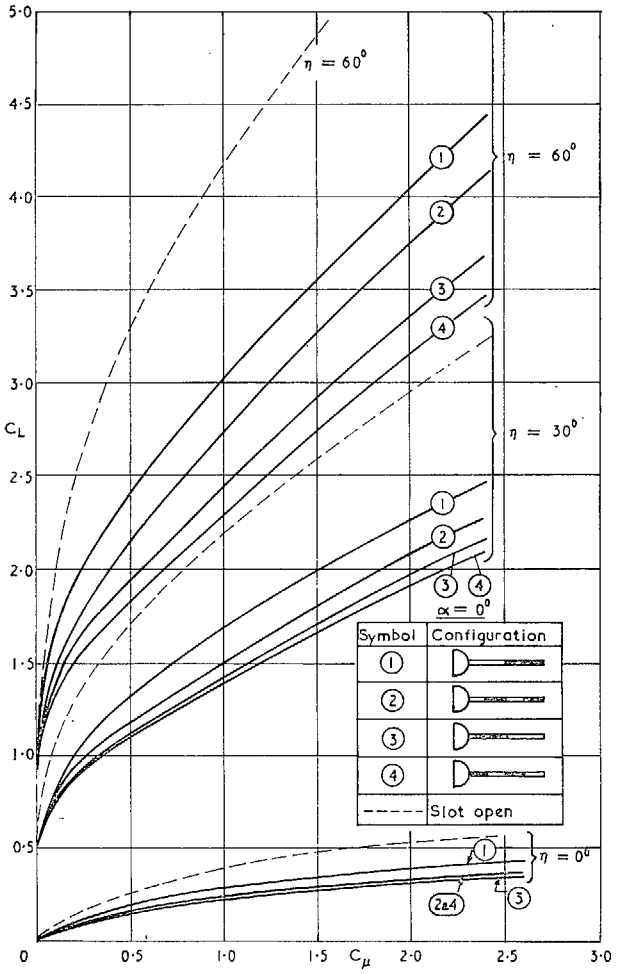

FIG. 6c. Lift for part-span blowing with full-span flap; $\alpha = 0°$.

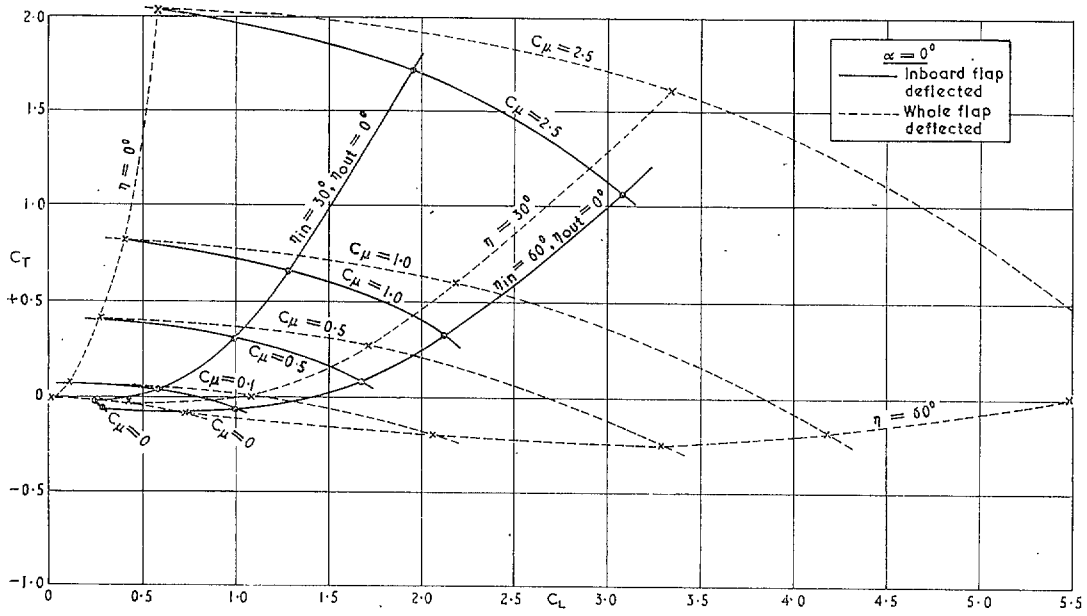

FIG. 7a. Variation of thrust with lift for part-span flap with full-span blowing, $\alpha = 0°$.

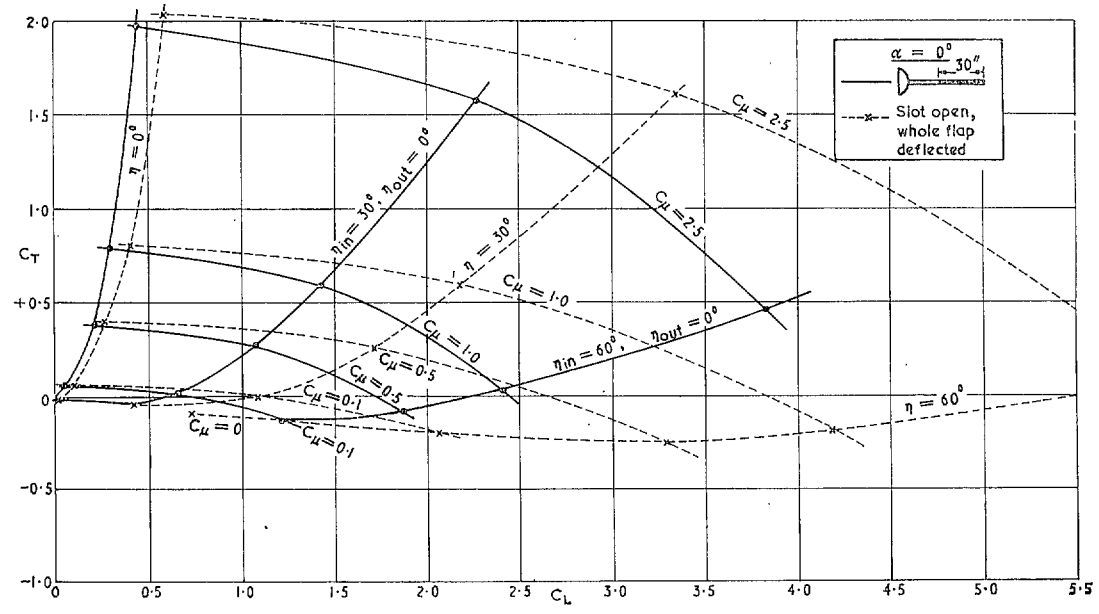

FIG. 7b. Variation of thrust with lift for blowing over inboard deflected flap only; $\alpha = 0°$.

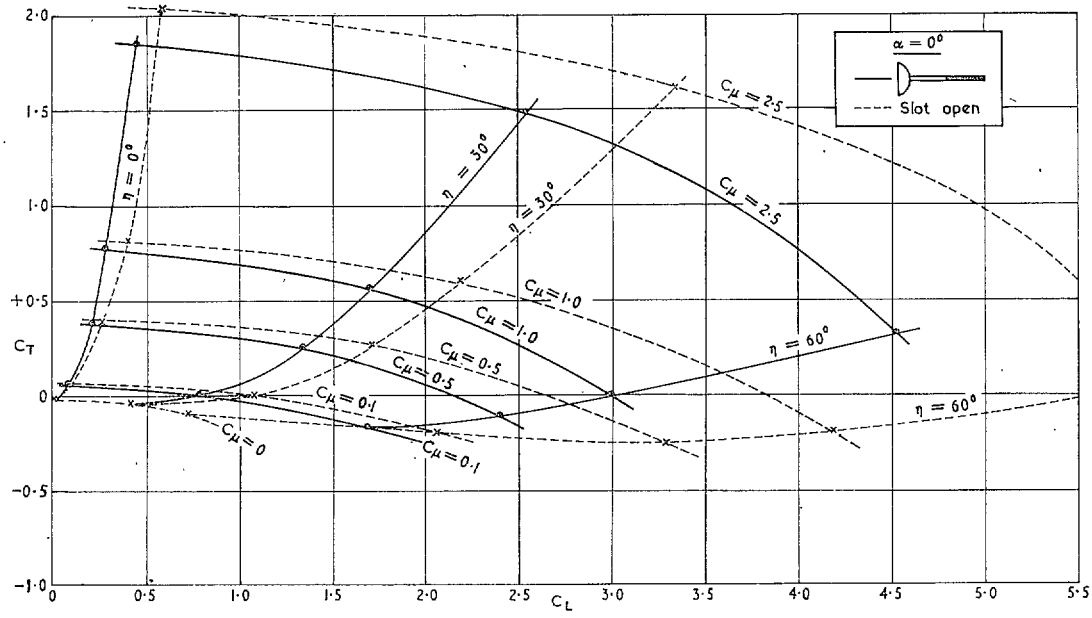

FIG. 7c. Variation of thrust with lift for part-span blowing and full-span flap; $\alpha = 0°$.

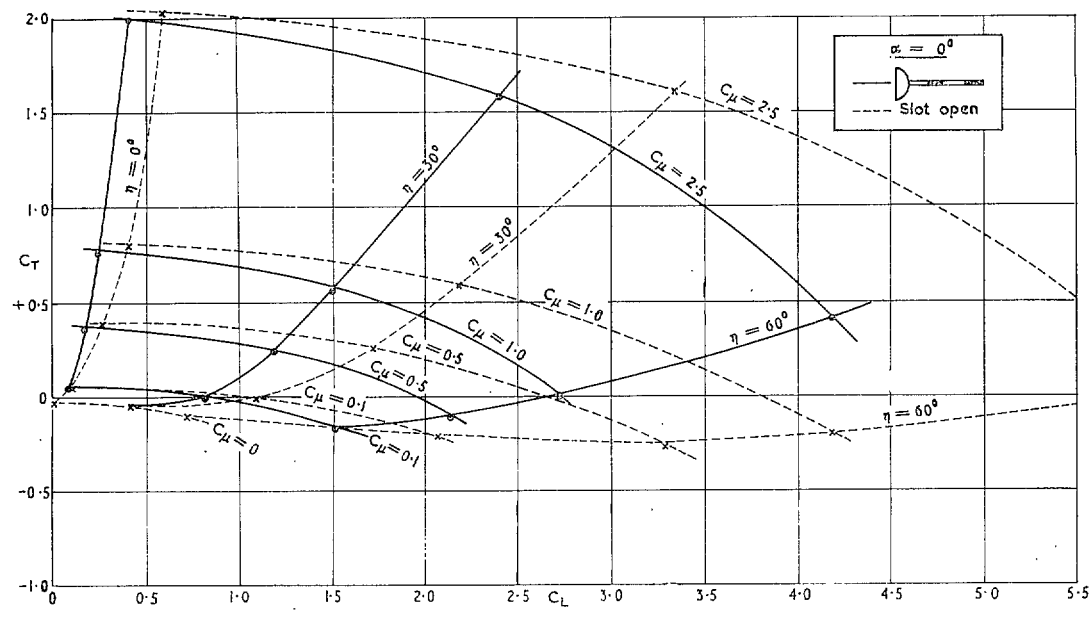

FIG. 7d. Variation of thrust with lift for part-span blowing and full-span flap; $\alpha = 0°$.

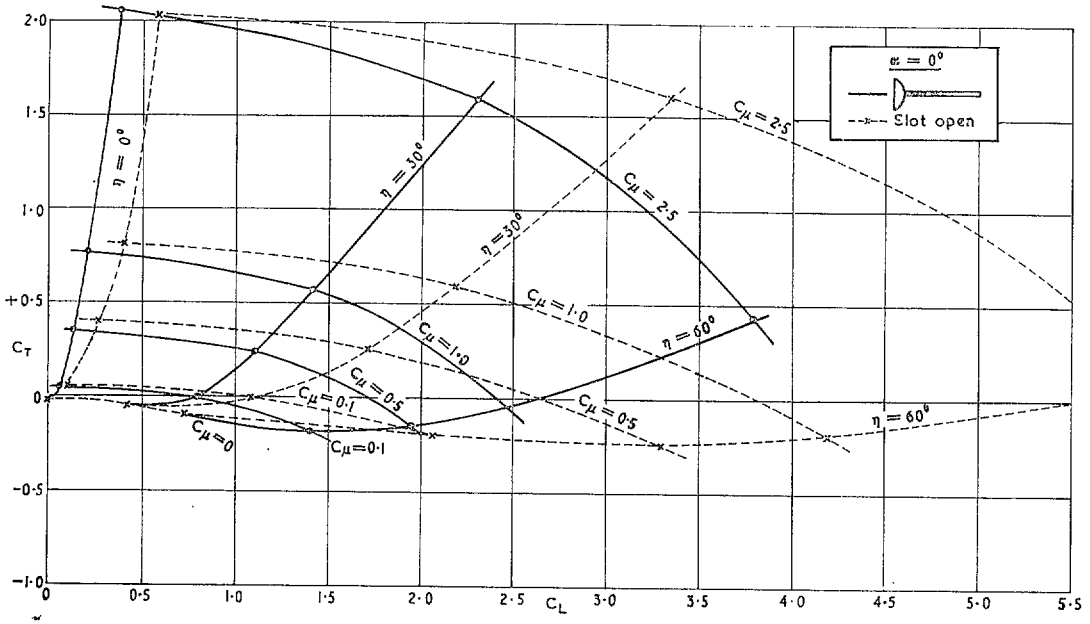

FIG. 7e. Variation of thrust with lift for part-span blowing and full-span flap; $\alpha = 0°$.

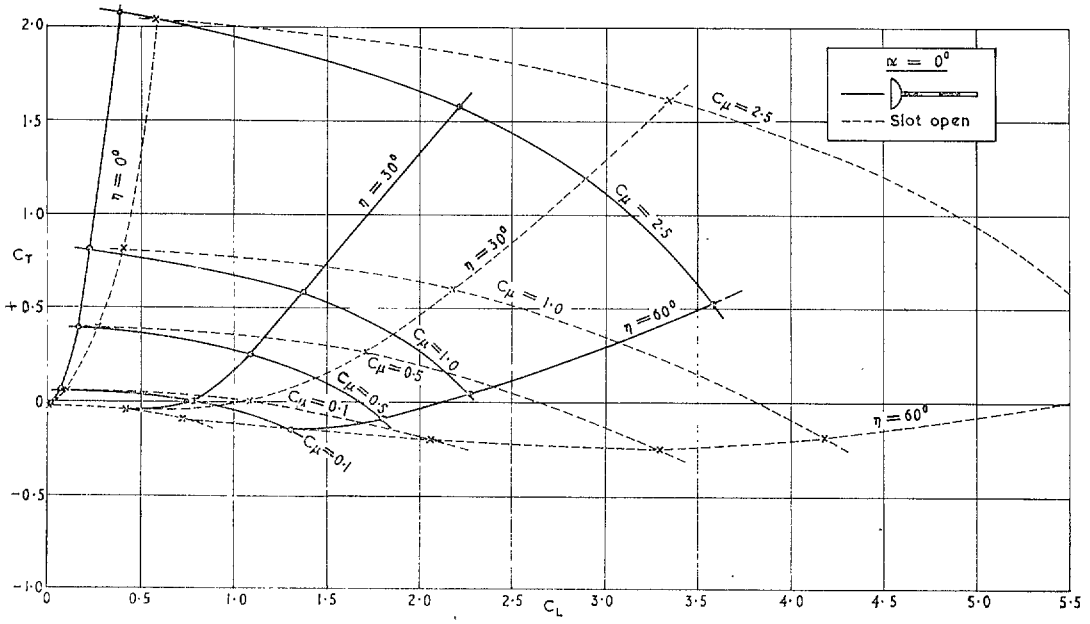

FIG. 7f. Variation of thrust with lift for part-span blowing and full-span flap; $\alpha = 0°$.

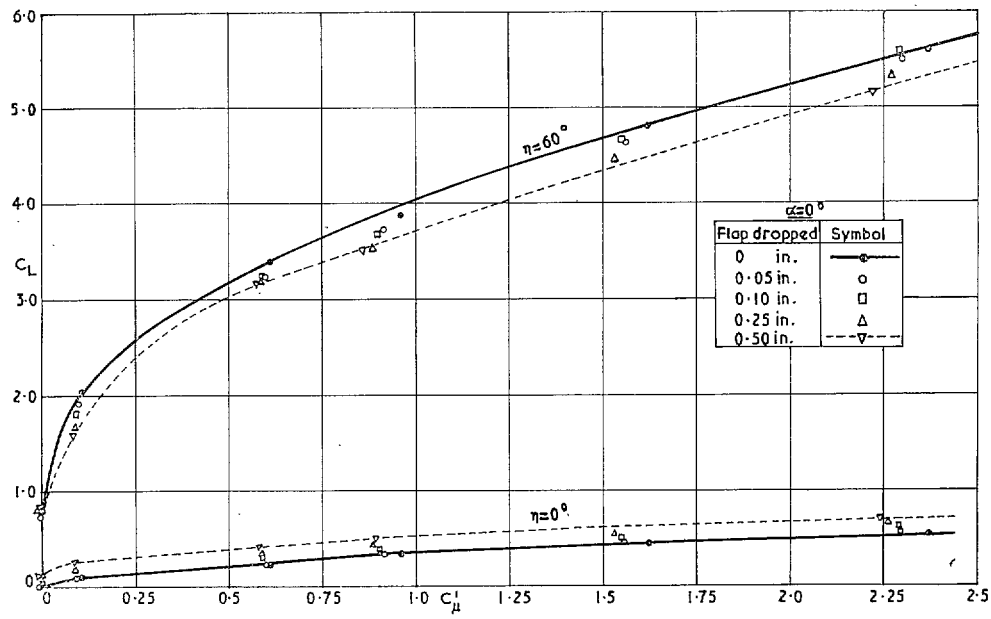

FIG. 8a. Flap-dropped tests: Variation of lift with momentum coefficient for $\alpha = 0°$.

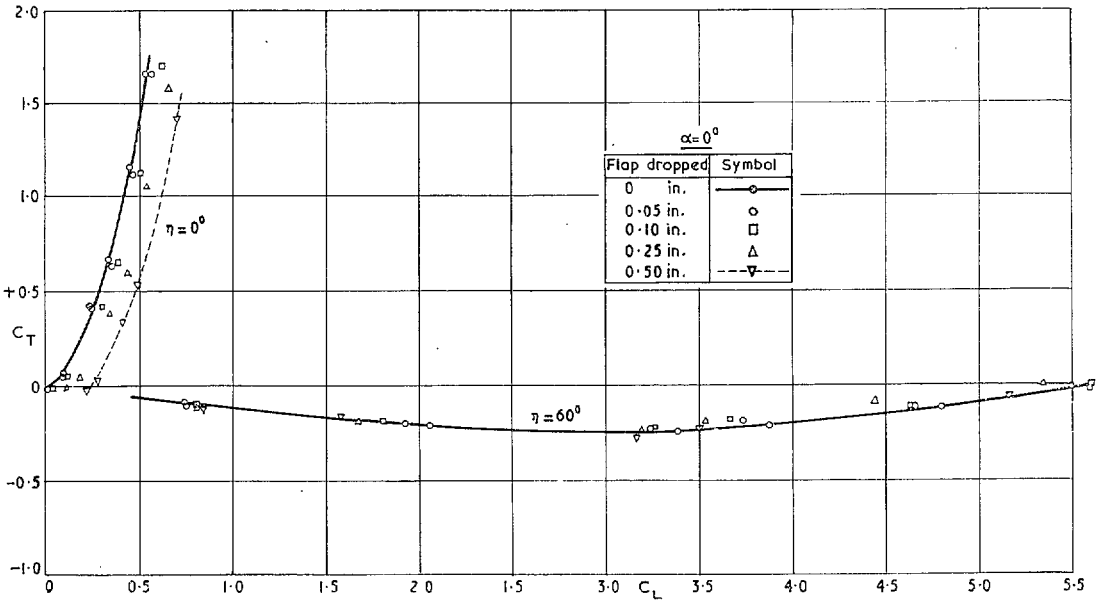

FIG. 8b. Flap-dropped tests: Variation of thrust with lift for $\alpha = 0°$.

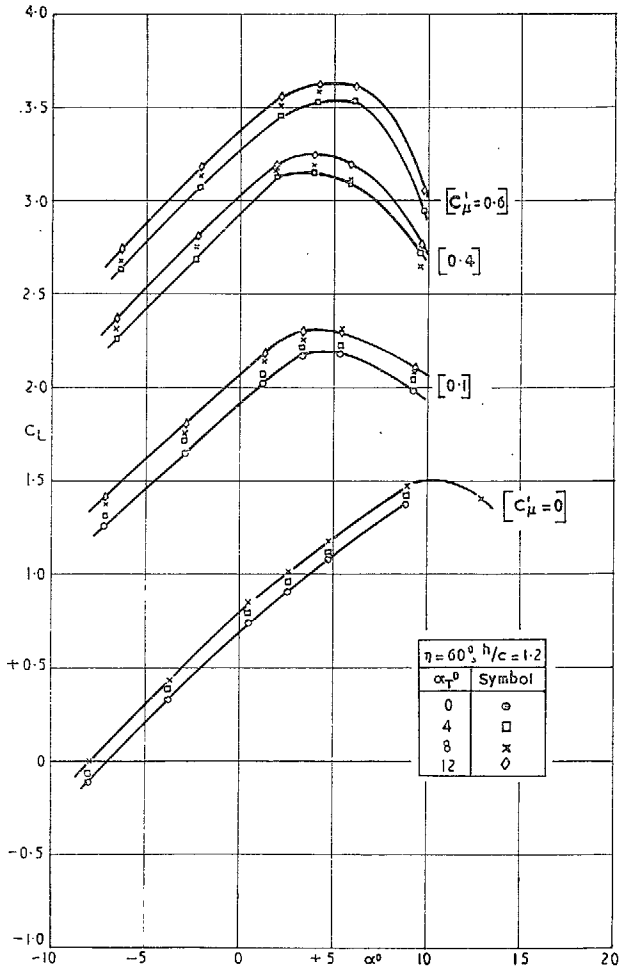

FIG. 9a. Variation of lift with incidence (tail on), for $\eta = 60°$, $h/c = 1·2$.

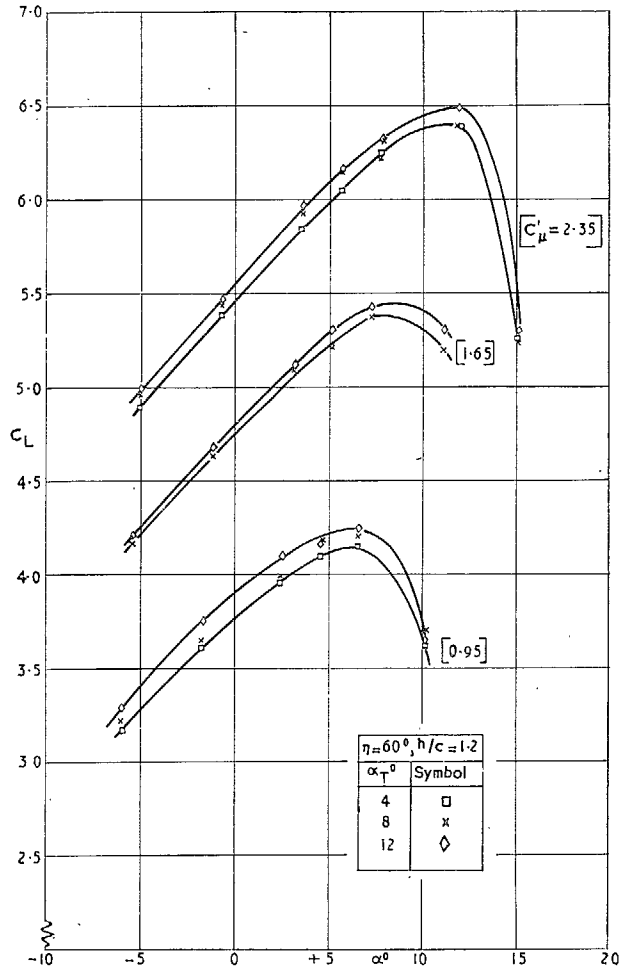

FIG. 9b. Variation of lift with incidence (tail on), for $\eta = 60°$, $h/c = 1·2$.

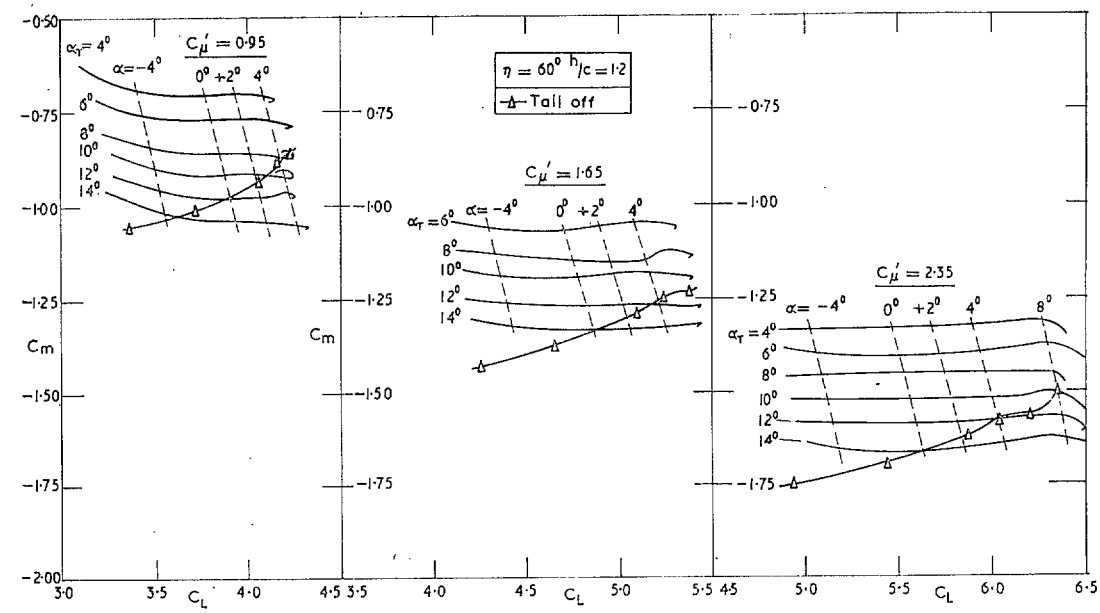

FIG. 10a. Variation of pitching moment with lift for $\eta = 60°$, $h/c = 1{\cdot}2$.

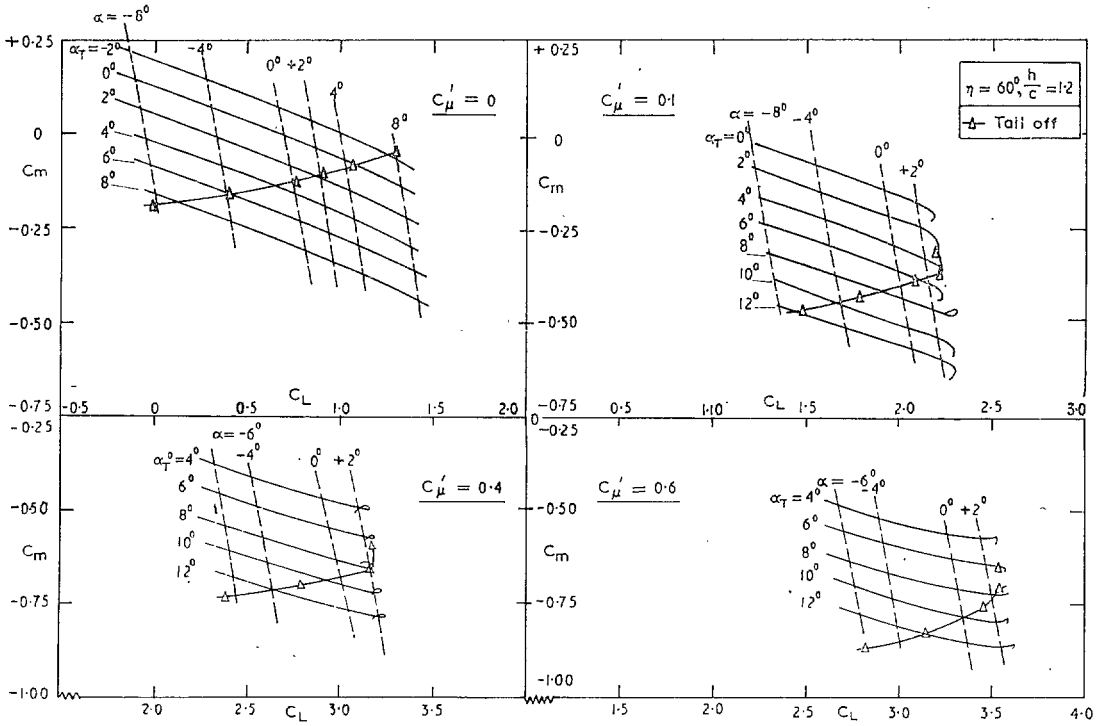

FIG. 10b. Variation of pitching moment with lift for $\eta = 60°$, $h/c = 1{\cdot}2$.

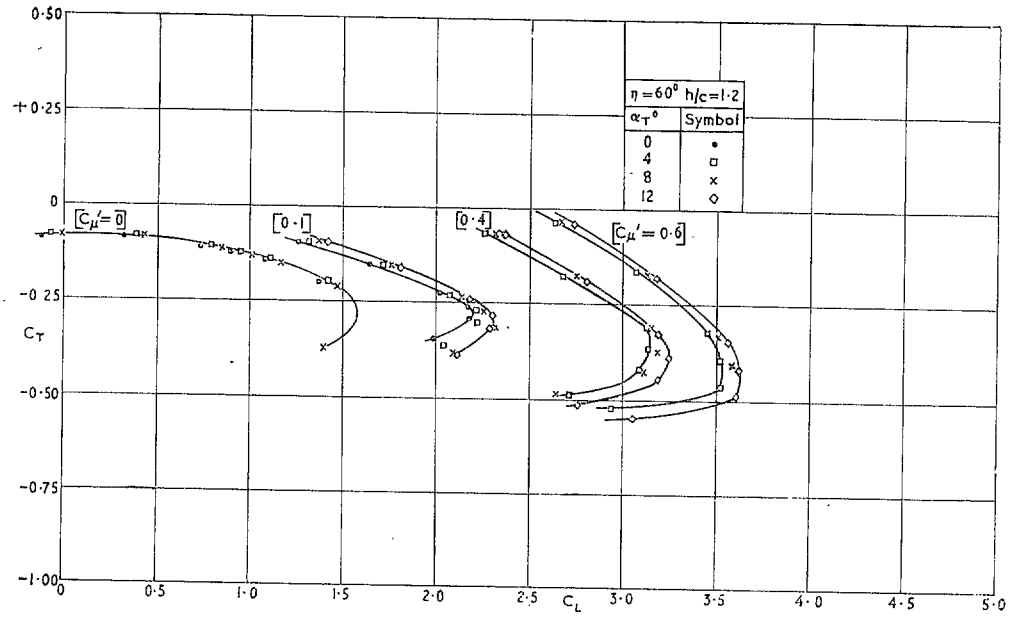

FIG. 11a. Variation of thrust with lift (tail on), for $\eta = 60°$, $h/c = 1 \cdot 2$.

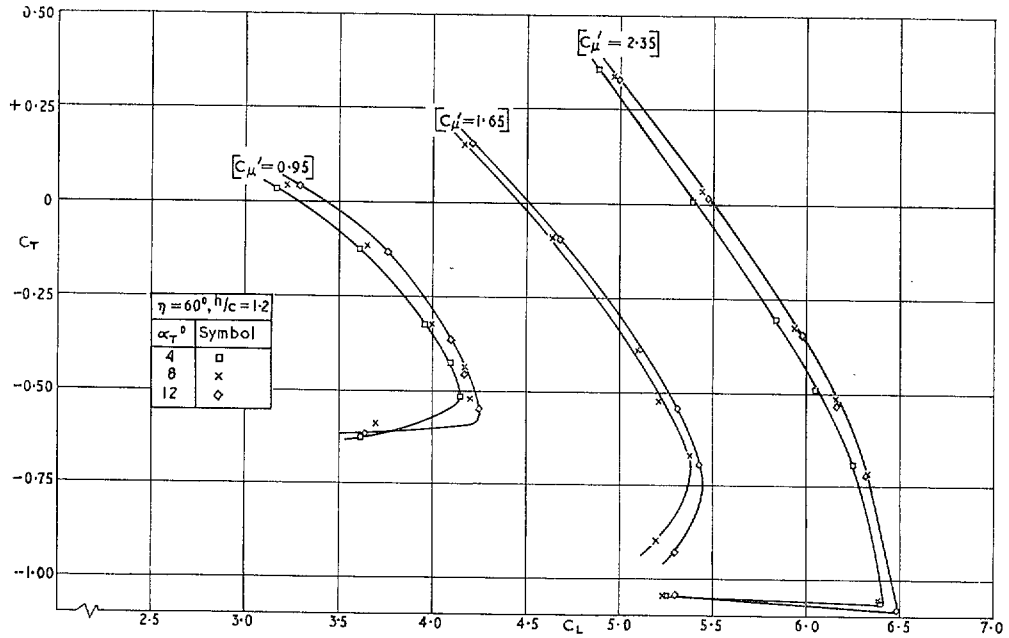

FIG. 11b. Variation of thrust with lift (tail on), for $\eta = 60°$, $h/c = 1 \cdot 2$.

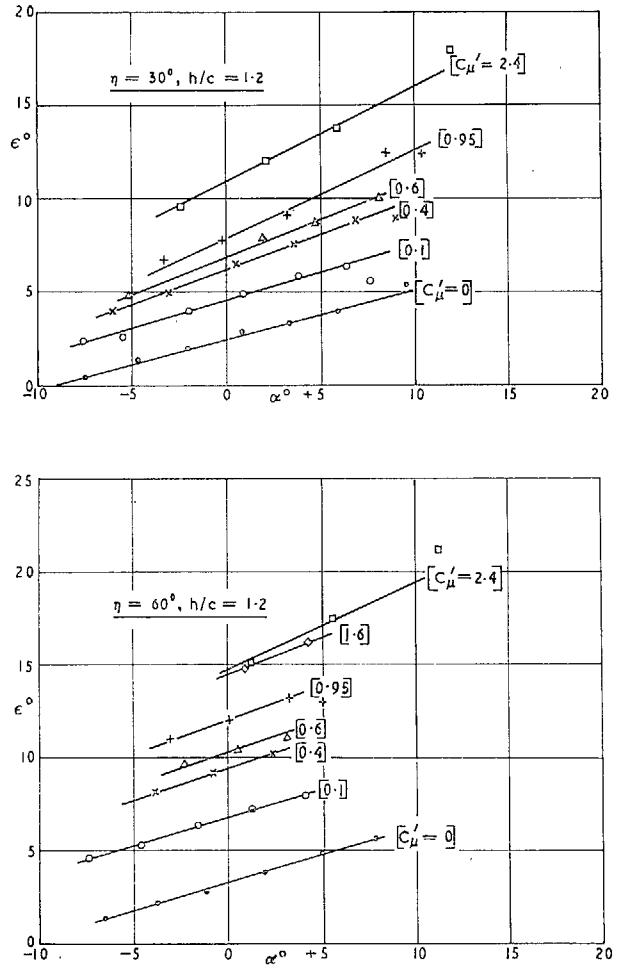

FIG. 12a. Variation of downwash with incidence for $h/c = 1 \cdot 2$.

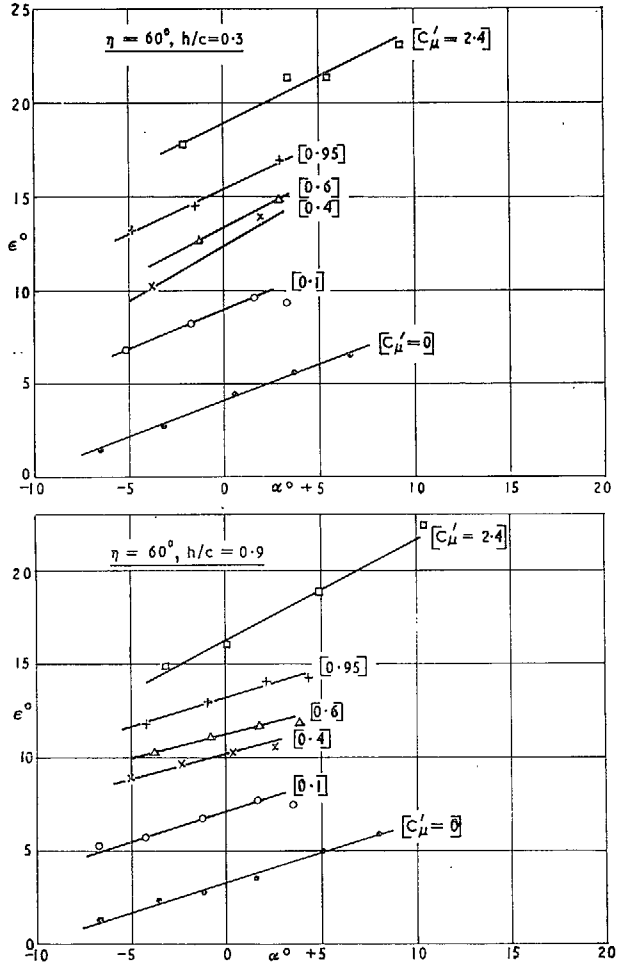

FIG. 12b. Variation of downwash with incidence for $\eta = 60°$.

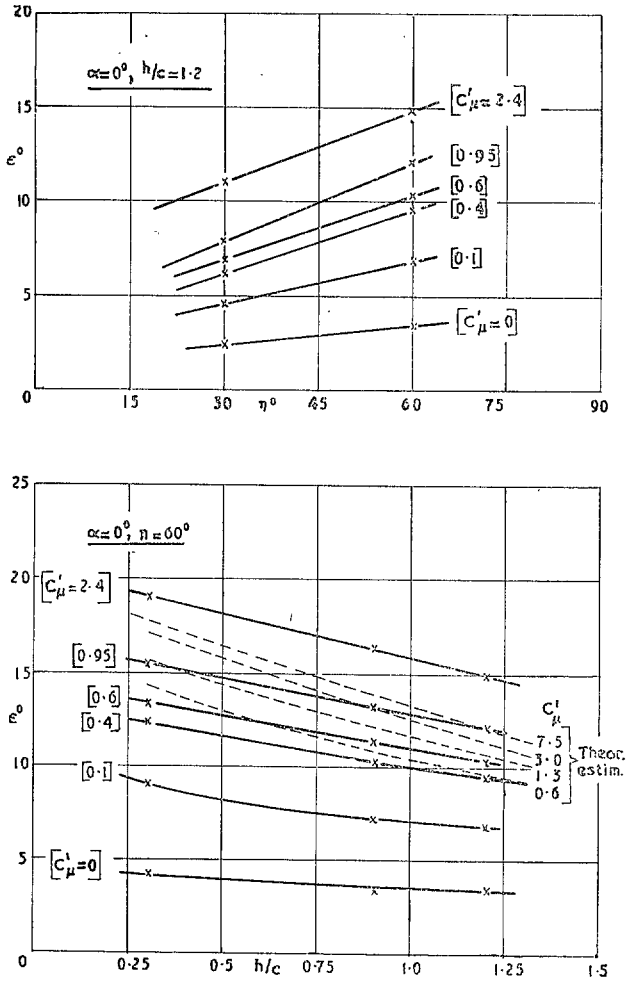

FIG. 13. Variation of downwash with tailplane height and flap angle, for $\alpha = 0°$.

(87355) Wt. 64/1857 K.5 3/64 Hw.

Publications of the Aeronautical Research Council

ANNUAL TECHNICAL REPORTS OF THE AERONAUTICAL RESEARCH COUNCIL (BOUND VOLUMES)

1942 Vol. I. Aero and Hydrodynamics, Aerofoils, Airscrews, Engines. 75*s.* (post 2*s.* 9*d.*)
Vol. II. Noise, Parachutes, Stability and Control, Structures, Vibration, Wind Tunnels. 47*s.* 6*d.* (post 2*s.* 3*d.*)

1943 Vol. I. Aerodynamics, Aerofoils, Airscrews. 80*s.* (post 2*s.* 6*d.*)
Vol. II. Engines, Flutter, Materials, Parachutes, Performance, Stability and Control, Structures. 90*s.* (post 2*s.* 9*d.*)

1944 Vol. I. Aero and Hydrodynamics, Aerofoils, Aircraft, Airscrews, Controls. 84*s.* (post 3*s.*)
Vol. II. Flutter and Vibration, Materials, Miscellaneous, Navigation, Parachutes, Performance, Plates and Panels, Stability, Structures, Test Equipment, Wind Tunnels. 84*s.* (post 3*s.*)

1945 Vol. I. Aero and Hydrodynamics, Aerofoils. 130*s.* (post 3*s.* 6*d.*)
Vol. II. Aircraft, Airscrews, Controls. 130*s.* (post 3*s.* 6*d.*)
Vol. III. Flutter and Vibration, Instruments, Miscellaneous, Parachutes, Plates and Panels, Propulsion. 130*s.* (post 3*s.* 3*d.*)
Vol. IV. Stability, Structures, Wind Tunnels, Wind Tunnel Technique. 130*s.* (post 3*s.* 3*d.*)

1946 Vol. I. Accidents, Aerodynamics, Aerofoils and Hydrofoils. 168*s.* (post 3*s.* 9*d.*)
Vol. II. Airscrews, Cabin Cooling, Chemical Hazards, Controls, Flames, Flutter, Helicopters, Instruments and Instrumentation, Interference, Jets, Miscellaneous, Parachutes. 168*s.* (post 3*s.* 3*d.*)
Vol. III. Performance, Propulsion, Seaplanes, Stability, Structures, Wind Tunnels. 168*s.* (post 3*s.* 6*d.*)

1947 Vol. I. Aerodynamics, Aerofoils, Aircraft. 168*s.* (post 3*s.* 9*d.*)
Vol. II. Airscrews and Rotors, Controls, Flutter, Materials, Miscellaneous, Parachutes, Propulsion, Seaplanes, Stability, Structures, Take-off and Landing. 168*s.* (post 3*s.* 9*d.*)

1948 Vol. I. Aerodynamics, Aerofoils, Aircraft, Airscrews, Controls, Flutter and Vibration, Helicopters, Instruments, Propulsion, Seaplane, Stability, Structures, Wind Tunnels. 130*s.* (post 3*s.* 3*d.*)
Vol. II. Aerodynamics, Aerofoils, Aircraft, Airscrews, Controls, Flutter and Vibration, Helicopters, Instruments, Propulsion, Seaplane, Stability, Structures, Wind Tunnels. 110*s.* (post 3*s.* 3*d.*)

Special Volumes

Vol. I. Aero and Hydrodynamics, Aerofoils, Controls, Flutter, Kites, Parachutes, Performance, Propulsion, Stability. 126*s.* (post 3*s.*)
Vol. II. Aero and Hydrodynamics, Aerofoils, Airscrews, Controls, Flutter, Materials, Miscellaneous, Parachutes, Propulsion, Stability, Structures. 147*s.* (post 3*s.*)
Vol. III. Aero and Hydrodynamics, Aerofoils, Airscrews, Controls, Flutter, Kites, Miscellaneous, Parachutes, Propulsion, Seaplanes, Stability, Structures, Test Equipment. 189*s.* (post 3*s.* 9*d.*)

Reviews of the Aeronautical Research Council

1939–48 3*s.* (post 6*d.*) 1949–54 5*s.* (post 5*d.*)

Index to all Reports and Memoranda published in the Annual Technical Reports

1909–1947 R. & M. 2600 (out of print)

Indexes to the Reports and Memoranda of the Aeronautical Research Council

Between Nos. 2351–2449	R. & M. No. 2450 2*s.* (post 3*d.*)
Between Nos. 2451–2549	R. & M. No. 2550 2*s.* 6*d.* (post 3*d.*)
Between Nos. 2551–2649	R. & M. No. 2650 2*s.* 6*d.* (post 3*d.*)
Between Nos. 2651–2749	R. & M. No. 2750 2*s.* 6*d.* (post 3*d.*)
Between Nos. 2751–2849	R. & M. No. 2850 2*s.* 6*d.* (post 3*d.*)
Between Nos. 2851–2949	R. & M. No. 2950 3*s.* (post 3*d.*)
Between Nos. 2951–3049	R. & M. No. 3050 3*s.* 6*d.* (post 3*d.*)
Between Nos. 3051–3149	R. & M. No. 3150 3*s.* 6*d.* (post 3*d.*)

HER MAJESTY'S STATIONERY OFFICE

from the addresses overleaf

Printed and published by
HER MAJESTY'S STATIONERY OFFICE

To be purchased from
York House, Kingsway, London w.c.2
423 Oxford Street, London w.1
13A Castle Street, Edinburgh 2
109 St. Mary Street, Cardiff
39 King Street, Manchester 2
50 Fairfax Street, Bristol 1
35 Smallbrook, Ringway, Birmingham 5
80 Chichester Street, Belfast 1
or through any bookseller

Printed in England

S.O. Code No. 23-3329